Hierarchical model for design and operation optimization of district cooling networks

Applied Energy 371 (2024) 123667

Contents lists available at ScienceDirect

Applied Energy

journal homepage: www.elsevier.com/locate/apenergy

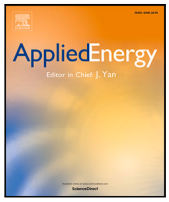

Hierarchical model for design and operation optimization of district cooling networks

Manfredi Neri [a,*], Elisa Guelpa [a], Jun Onn Khor [b], Alessandro Romagnoli [c], Vittorio Verda [a]

[a] Department of Energy DENERG, Polytechnic University of Turin, Italy
[b] Energy Research Institute @ NTU, Nanyang Technological University, Singapore
[c] School of Mechanical and Aerospace Engineering, Nanyang Technological University, Singapore

ARTICLE INFO

Keywords:
District cooling
Thermal network
Genetic algorithm
MILP

ABSTRACT

District cooling systems offer a promising alternative to conventional cooling, thanks to overall larger efficiencies and reduced carbon footprint. On the other hand they are characterized by large capital and operational costs that impede their diffusion. Optimizing the design and operation of these systems is therefore fundamental to fully exploit their potential. This paper proposes a novel optimization framework for the simultaneous optimization of design and operation of these systems. The model integrates a genetic algorithm at a master level with Mixed Integer Linear Programming models at a lower level. This approach enables the optimization of various aspects, including network topology, plant locations, supply temperatures and the selection of thermal storage technology. The study showed that in the specific case of Singapore, where the cost for space occupancy is significant, latent heat thermal storages are preferred. In addition, the results highlighted the cost benefits of thermal storage, as district cooling networks lacking it can be from 6.2% to 20.8% more expensive, depending on the scenario. Furthermore, the study demonstrated that the utilization of waste heat through absorption chillers enhances the economic feasibility of district cooling, lowering the payback time by up to 5 years. Lastly, it was observed that 3 °C increase of the indoor set point temperature could reduce the payback time by 3 years and increase the final net present value by 43%, as larger network supply temperatures allow chillers to operate with better performances. The developed model allows to estimate various crucial outcomes with few input parameters, representing a useful tool for both research and planning.

1. Introduction

Space cooling accounts for 20% of building electricity consumption and is responsible for 1 Gton of CO_2 emissions every year [1]. Over the past three decades the demand has increased by more than three times, being one of fastest increasing energy-end-use sectors. According to the International Energy Agency (IEA), in the next 30 years cooling demand will increase by 100% and 2/3 of households will be equipped with air conditioning [1,2]. The main driving factors for the increase in cooling demand are the increased accessibility to these systems, compared to the past and the changes in weather conditions due to global warming. During the summer, electricity peak demand is highly driven by the cooling demand, especially during heat waves. In hot countries, cooling can be responsible for about 30% of peak electricity demand and, by 2050, it could reach 50%. IEA [1] stated that space cooling is one of the energy sectors which still require major actions to reach the goal of Net Zero emissions by 2050.

District cooling is an interesting alternative to conventional cooling systems in locations with high energy density, such as urban areas. These systems generally have higher efficiencies, since larger industrial chillers typically have better performances than the smaller ones. In addition, the demand of district cooling systems tends to be more homogeneous than the demand of a single building, due to a diversification of the demand. As a consequence, the demand peaks do not coincide and therefore the collective peak demand of a district cooling system is lower compared to combined demand peaks of all buildings [3]. This allows to avoid chillers oversizing and to reduce their investments. In addition, when the chillers are operated with a more homogeneous load, they work closer to design conditions, with overall better performances [4]. Moreover, further energy savings can be achieved when integrated with free cooling sources such as water basins or waste heat from industrial processes by means of absorption chillers [5,6]. Coupling district cooling with high efficient systems that exploit available local sources, such as groundwater heat pumps also allows to reduce both operational and capital costs [7]. Integrating DC systems with thermal energy storage can also reduce pressure on the electricity system and lower operation costs, by charging the storages

* Corresponding author.
E-mail address: manfredi.neri@polito.it (M. Neri).

https://doi.org/10.1016/j.apenergy.2024.123667
Received 31 January 2024; Received in revised form 26 May 2024; Accepted 6 June 2024
Available online 17 June 2024

Nomenclature

Acronyms

MILP	Mixed Integer Linear Programming
NPV	Net present value
PCM	Phase change material
PLR	Partial Load Ratio
STES	Sensible thermal energy storage

Chiller performance curves

a, b, c, d, e, f, g	Coefficients used in the correction functions
$C_{chiller}$	Chiller cooling capacity
COP_{ref}	Chiller COP at full load
f_T	Supply temperature correction factor
f_{PLR}	Partial Load correction factor
P_{ref}	Electrical power required by the chiller at full load

Cost function terms

$cost^{cap}_{ch,ind}$	Capital cost of individual chillers
$cost^{occ}_{ch,ind}$	Space occupancy cost of individual chillers
$cost^{op}_{ch,ind}$	Operation cost of individual chillers
$cost^{cap}_{ch}$	Capital cost of centralized chillers
$cost^{occ}_{ch}$	Space occupancy cost of centralized chillers
$cost^{op}_{ch}$	Operation cost of centralized chillers
$cost_{piping}$	Piping cost
$cost_{pumping}$	Pumping cost
$cost^{cap}_{st}$	Capital cost of storages
$cost^{occ}_{st}$	Space occupancy cost of thermal storages

Auxiliary variables

Δp^t_{ij}	Pressure drop on the pipe that connects nodes i and j
ΔP^t_i	Pressure difference between supply and return lines on node i
$G^t_{ext,i}$	Mass flow rates entering or exiting from node i
G^t_{ext}	Vector of mass flow rates entering or exiting from the network
P_{pump}, w^t	Pumping power required at time t by plant w
z^m_{ij}	Binary variable that indicates if diameter D^m is installed in branch (i, j)

Indices

(i, j)	Generic branch of graph
i, j	Generic nodes of graph
k	Generic compression chiller
m	Generic pipe size
t	Generic time instance
u	Generic building
w	Generic plant

Master problem decision variables

$\theta_{ch,s}$	Network supply temperature
$vmax_m$	Design velocity for pipes with generic commercial diameter m
x_u	Integer variables that indicate by which chiller, the demand of building u is satisfied

Design and operation optimization of chillers and storages subproblem variables

$C^t_{Ice,w}$	Residual capacity of ice thermal storage at time t in plant w
$C^t_{PCM,w}$	Residual capacity of PCM thermal storage at time t in plant w
$C^t_{STES,w}$	Residual capacity of sensible storage at time t in plant w
$MaxQ_{ch,st,w}$	Maximum cooling power that can be produced at lower temperature levels in plant w
$N_{abs,w}$	Number of installed absorption chillers in plant w
$N^k_{ch,st,w}$	Number of chillers of size k that can produce cooling water at lower temperature levels in plant w
$N^k_{ch,w}$	Number of installed chillers of size k in plant w
$Q^t_{abs,w}$	Cooling produced by absorption chillers at time t in plant w
$Q^t_{ch,0,w}$	Cooling power produced at nominal supply temperature $\theta_{ch,s}$ at time t in plant w
$Q^t_{ch,PCM,w}$	Cooling power produced at the temperature level required by PCM thermal storage at time t in plant w
$Q^t_{ch,PCM,w}$	Cooling power produced at the temperature level required by ice thermal storage at time t in plant w
$Q^t_{ch,w}$	Total cooling power produced by compression chillers at time t in plant w
$Q^t_{Ice,w}$	Cooling power stored/released by ice thermal storage at time t
$Q^t_{PCM,w}$	Cooling power stored/released by PCM thermal storage at time t in plant w
$Q^t_{STES,w}$	Cooling power stored/released by sensible thermal storage at time t in plant w
$S_{Ice,w}$	Maximum capacity of ice thermal storage in plant w
$S_{PCM,w}$	Maximum capacity of PCM thermal storage in plant w
$S_{STES,w}$	Maximum capacity of sensible thermal storage in plant w
$x^t_{Ice,w}$	Binary variable that indicates if ice thermal storage is charged at time t in plant w
$x^t_{PCM,w}$	Binary variable that indicates if PCM is charged at time t in plant w
$y_{Ice,w}$	Binary variable that indicates if ice thermal storage is installed in plant w

$y_{PCM,w}$	Binary variable that indicates if PCM thermal storage is installed in plant w
$y_{STES,w}$	Binary variable that indicates if sensible thermal storage is installed in plant w

Parameters

Δt	Time interval between two time-steps
ρ	Water density
A	Incidence matrix
c_k	Capital cost of chiller of size k
c_{abs}^{cap}	Capital cost of absorption chiller
c_{abs}^{OM}	Operational and maintenance cost per unit of cooling energy produced by absorption chiller
$c_{ch,ind}^{u}$	Capital cost of individual chillers to be installed in building u
c_{el}^{t}	Electricity cost at time t
$c_{ETS,u}$	Capital cost of energy transfer station in building u
c_{Ice}	Capital cost to install a ice thermal storage of unitary capacity
c_{occ}	Unitary space occupancy cost
c_{PCM}	Capital cost to install a PCM thermal storage of unitary capacity
c_{pipe}^{m}	Unitary cost of pipe with commercial diameter m
c_{STES}	Capital cost to install a sensible thermal storage of unitary capacity
COP_u^t	COP of individual chillers installed at building u at time t
COP_0^t	COP of compression chiller producing chilled water at the temperature $\theta_{ch,s}$
COP_{abs}^t	COP of absorption chiller at time t
COP_{Ice}^t	COP of compression chiller charging ice thermal storage at time t
COP_{PCM}^t	COP of compression chiller charging PCM at time t
F	Sufficiently large number used in big-M constraints
f	Friction coefficient
$Gmax_{ext}^{j}$	Maximum net flow rate entering or exiting from node j
L_{ij}	Length of the edge that connects node i with node j
N_y	Project lifetime in years
n_d	Number of utilization days
Q_w^t	Cooling demand that must be satisfied at time t by plant w
Q_u^t	Cooling demand of building u at time t
$Q_{waste-heat}$	Available waste heat
r	Interest rate
s_{abs}	Space occupied by an absorption chiller
s_{abs}	Space occupied by absorption chiller
$S_{ch,ind}^{u}$	Chiller capacity installed in building u
$S_{ch,ind}^{u}$	Total capacity of individual chillers installed in building u
$s_{ch,ind}^{u}$	Space occupied by the individual chillers installed in building u
s_{ICE}	Space occupied by ice thermal storage per unit of installed capacity
s_k	Space occupied by chiller of size k
s_{PCM}	Space occupied by PCM thermal storage per unit of installed capacity
s_{STES}	Space occupied by sensible thermal storage per unit of installed capacity

Sets

E	Set of all possible branches of the graph
H	Set of possible plant nodes
K	Set of types of compression chillers
M	Set of possible pipe sizes
T	Set of time instances
U	Set of all buildings
V	Set of all nodes of the graph
V^j	Set of nodes adjacent to node j

Topology optimization variables

$Gmax_{ij}^{+}$	Positive part of maximum mass flow rate flowing in branch (i,j)
$Gmax_{ij}^{-}$	Negative part of maximum mass flow rate flowing in branch (i,j)
z_{ij}^{+}	Binary variable that indicates if branch (i,j) is selected
z_{ij}^{-}	Binary variable that indicates if branch (j,i) is selected

when the demand is smaller and discharging them during demand peaks [8]. In addition, using thermal storage for peak shaving and valley filling reduces the required chiller capacity and, consequently, the capital costs [9]. Compared to district heating, this technology is characterized by larger capital and pumping costs, since higher mass flow rates are required to transfer the same amount of energy, due to the lower temperature difference between supply and return lines [10,11].

Optimization tools can help to minimize the costs and fully exploit the potential of district cooling. Different models have been developed for the design and operation optimization of district cooling systems. The most common approaches include Mixed Integer Linear Programming and the use of evolutionary algorithms [12–14]. In the context of operation optimization of district heating and cooling systems, different authors implemented optimization approaches based on both physical and data-driven models. Chiam et al. [15] developed a hierarchical tool that integrates an MILP model and a genetic algorithm, to optimize the hourly operation of district cooling systems. The framework takes into account the performance curves of different components that are connected to each other and finds the optimal set-points that minimize the total costs. Yan et al. [16] implemented a non linear model to optimize the operation of district cooling systems, modelling the spatio-temporal cooling demand, the cooling dissipations and the power consumption of different components. Tang et al. [17] implemented a model predictive control strategy to optimize the operation of a district cooling network with ice thermal energy storage. The implemented model allowed to reduce operating costs by 8% compared to conventional operation strategies. Chen et al. [18] developed a physical model of an ice thermal storage coupled with a water cooled chiller in a district cooling system and optimized its operation by means of a genetic algorithm. Cox et al. [19] implemented a model predictive control based on neural networks to optimize the operation of a district cooling network with

ice thermal storage. The results showed that the strategy can effectively adapt to varying loads and electricity tariff, saving up to 17% of operating costs.

Concerning the design of district cooling systems, different authors proposed models to optimize the network layout, the pipe diameters, the buildings to be connected, the positions of chillers and storages. Pipe diameter optimization is fundamental, as a large diameter increases piping costs, while lower diameters are responsible for higher pressure drops and therefore pumping costs. Moreover, a larger diameter is also responsible for higher heat gains from the ground, that cause an increase of the supply temperature to the final users. With this regard, Coz et al. [20] optimized the diameter and insulation thickness of the pipes in a district cooling network, minimizing the exergy cost.

Other authors combined the optimization of diameters with network layout and the position of chillers and storages. Guelpa et al. [21] developed a genetic algorithm to optimize the position of chillers in a district cooling network with the goal of minimizing the total costs. Al-Noaimi, Khir and Haouari [22,23] developed MILP models to optimize both the topology and the position of chillers and storages in a district cooling system. They handled the non-linearities with reformulation techniques and decomposed the problem, optimizing the design and operation of chillers and storages separately from the network topology and pipe sizes. Dorfner et al. [24] optimized the network layout and pipe diameters with a MILP model, including also redundant constraints and the possible unavailability of chiller plants. Lambert et al. [25] developed a multistage stochastic programming model to optimize multiple design phases of district heating networks. Shi et al. [26] studied the impact of street layouts on the feasibility of district cooling networks, considering different cost indicators. They studied the impact of the block area, block elongation and site area, considering real data from five districts in Singapore. They found that block area is the parameter with the highest impact on the cost indicators. Neri et al. [27] implemented a Mixed Integer Quadratic Constrained Programming to simultaneously optimize the pipe diameters, the position and capacity of chillers and storages and the operation strategy. They found that if demand is seasonal, it is sufficient dimensioning the chillers on the base of the average daily demand, using the storages only for peak shaving and valley filling. On the other hand, if demand is present all year round, it is necessary optimizing the design and operation simultaneously, especially, if there is a large daily variation of electricity price.

Some authors focused also on the selection of the buildings to be connected to a district cooling network. Chow et al. [3] optimized the set of building types to be connected to a district cooling network with the goal of minimizing the contemporaneity factor with the consequent increase of chillers performances and reduction of their sizes. Other authors instead optimized the specific buildings to be connected, based on the economic feasibility. Bordin et al. [28] developed a model based on an MILP approach to optimize the expansion of a district heating network. They approximated pressure drops by using piecewise linearization. Neri et al. [29] optimized the topology and the set of buildings to be connected to a district cooling system, implementing both an MILP model and genetic algorithm and showed how the second approach outperforms the first in terms of computational cost. They also implemented a stochastic approach [30] in order to optimize the network topology under demand and cost uncertainty. The model optimizes the initial layout, the pipe diameters and the set of buildings to be connected, taking into account for possible future network expansions.

Other authors focused on the chiller and storage design rather than on the network topology, trying to combine the optimization of design and operation. Alghool et al. [31] implemented an MILP model for the design and operation optimization of DC systems integrated with solar cooling technologies. Ismaen et al. [32] developed an optimization framework for district cooling systems with multiple chillers. Their tool enables the optimization of design and operation of the chillers minimizing total costs while satisfying different system requirements expressed as constraints. The results showed that when cooling demand is variable it is more convenient installing chillers with multiple capacities, in order to operate them with better performances. Hsu et al. [33] implemented a dynamic programming model to optimize the design and operation of island district cooling systems integrated with waste heat from diesel generators. They optimized the sizes of the absorption chiller and the thermal storage. The results showed a payback time of four years for the district cooling investments. Mazzoni et al. [34] developed an optimization framework for energy systems and applied it to the case study of a Singapore district cooling network. They optimized the design of chiller and thermal energy storage, considering different available technologies. The results showed, that due to the large space occupancy costs, ice thermal storage is more feasible, thanks to the higher volumetric capacity. Zaw et al. [35] realized a framework for the optimal design and operation of district cooling systems based on the interior point method. They applied the model to the Singapore case study and from the results emerged that the tool can bring up to 21% of savings in terms of total life cycle costs. Gang et al. [36] proposed a robust optimization approach for the design of district cooling networks, which takes into account the uncertainty related to cooling demand and equipment reliability. Wirtz et al. [37] implemented two approaches to optimize the multiperiod design of district heating and cooling systems. The results showed that compared to single period models, these approaches can provide up to 17% of cost savings. Wirtz also developed a web-based planning tool for designing district heating and cooling networks [38]. The platform, by means of a linear optimizer allows to design and dimensionate the technologies to be installed, taking into account the possible integration with renewable energy sources. He et al. [39] proposed a multi-objective optimization model to select the capacity and configuration of chillers in a district cooling network, considering multiple cooling scenarios. They applied the model to the district cooling network of Guangdong and estimated that it would allow to save up to 11% in terms of operating costs, thanks to the reduction of chillers operation at partial load conditions.

The existing studies that compare district cooling networks with traditional systems are based on the assumption that district cooling systems are more efficient, thanks to the installation of larger industrial chillers. If on one hand this may be true for buildings with small cooling demand, where chillers with smaller capacities are installed, on the other hand, this may not be the case for buildings with very large cooling demand, such as malls or offices. Indeed, in these buildings it is possible to have large efficient chillers installed, without the need to connect them to a district cooling network. In these cases the economic advantages of district cooling systems compared to individual cooling solutions are less obvious. However, district cooling can still be feasible for different reasons. The first is that the operation of chillers in district cooling systems is closer to design conditions, thanks to the installation of multiple capacities that reduce as much as possible chiller operation at partial load. The second is that larger centralized chillers tend to occupy less space than smaller ones. Therefore, district cooling can help reducing space occupancy, which in the major cities can represent a non-negligible cost. The third reason is that district cooling networks can be easily integrated with renewable energy sources, such as free cooling from water basins or waste heat from industrial processes.

In this paper we address this gap by optimizing the design and operation of a district cooling network in a neighbourhood of Singapore, characterized by commercial and office buildings with large cooling demand. The main novelty of this paper consists in a new framework able to optimize a wide set of design and operation variables. Compared to the models already available in literature, which focus on few design variables, this tool indeed optimizes multiple aspects related to the design and operation of district cooling networks. In particular, it has the objective of minimizing the overall costs, optimizing: (a) the network topology, (b) the hourly operation of chillers and storages, (c) their capacities and (d) their locations. In addition, the model addresses the optimization of network supply temperature and the

type of storage technology taking into account the effect they have on chiller efficiency, space occupancy and on pumping costs. Indeed, sensible thermal storage may allow chillers to operate more efficiently at higher temperatures, but has lower volumetric capacity. On the other hand, ice thermal storage or other commercial phase change materials require lower space, but also lower supply temperature to be charged, leading to lower chiller efficiencies. Combining all these aspects allows to fully exploit the potential of this technology and to increase the competitiveness of district cooling compared to other technologies.

In addition, by applying the model to the Singapore case study under different scenario conditions, the paper aims to provide useful design guidelines and insights that can help decision makers in planning and assessing the feasibility of future district cooling systems. In particular, we studied the benefits achievable by increasing the indoor set point temperature, while respecting the guidelines for thermal comfort conditions. It was also analysed how the presence of waste heat can influence the optimal topology and enhance district cooling potential, reducing the total costs and the payback time. Lastly, the influence of peak electricity cost and space occupancy cost on the optimal network topology and on the design and operation of chillers and storages was also examined.

2. Methodology

The objective of the model is to optimize the design and operation of district cooling systems, minimizing the total overall costs, characterized by the sum of capital and operation expenditures. In particular, the model optimizes the following aspects:

- the set of buildings to be connected;
- the pipe diameters and network topology;
- the position of production plants;
- the capacity and hourly operation of chillers and storages;
- the type of storage technology;
- the network supply temperature.

The model is based on a hierarchical structure, characterized by a master problem at superior level and two groups of subproblems at inner level. The master problem is solved by a genetic algorithm that finds iteratively the optimal values of its variables, and at each iteration the subproblems are solved by means of Mixed Integer Linear Programming models. The goal of the genetic algorithm is to find the optimal set of buildings to be connected to the district cooling network, the location of the plants, the supply temperature and the maximum velocity admissible in each commercial diameter. The goal of the first class of subproblems is to optimize the capacity and operation of chillers and storages in each plant. As a consequence, for each plant an MILP problem is solved to find the optimal capacity of chillers and storages and the daily operation. The goal of the second subproblem is instead to optimize the network topology, providing as output the tree-network with the shortest total length. The subproblems are solved, fixing the master problem variables. The latter are varied iteratively through the genetic algorithm and at each iteration the values of the variables are used as input parameters to solve the two classes of subproblems, whose outputs are needed to compute the master problem cost function. The model has therefore a nested structure, where the outer part is characterized by the master problem. The flowchart of the hierarchical model is shown in Fig. 1.

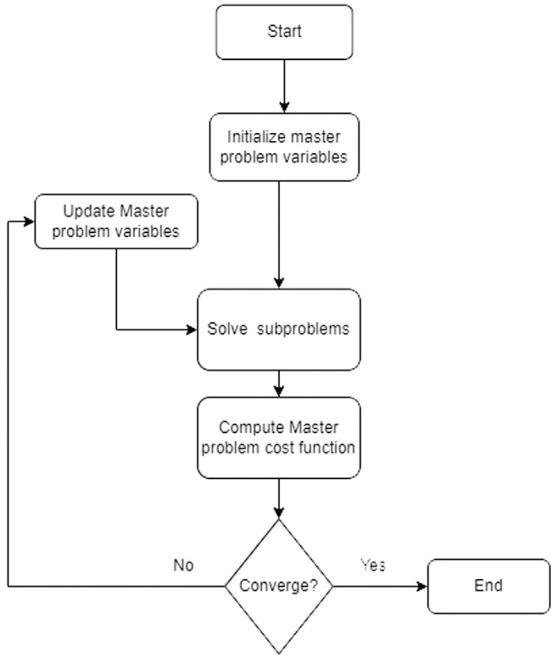

Fig. 1. Hierarchical model flowchart.

2.1. General assumptions

The whole hierarchical model is based on the following assumptions.

- Different plant locations can be selected and each of them includes chillers and, eventually, thermal storages.
- Heat gains in pipes are neglected due to the low temperature difference between the network and the ground.
- The demand of each building is always satisfied by a specific plant. This assumption is based on the idea that the demand of buildings is satisfied by plants close to them, in order to reduce the pumping costs. This assumption simplifies the problem, allowing to optimize separately each plant. Indeed the production of each plant is independent and separate from the others, since it is bounded to the demand of the buildings that it must satisfy.
- When varying the network supply temperature, the heat transfer areas of heat exchangers are assumed to be constant. It is assumed that the logarithmic average temperature difference between the secondary and primary loops can be considered constant. Consequently, if network supply temperature increases, the return temperature decreases to maintain the same logarithmic temperature difference with the secondary loop. As a consequence, if temperature supply increases, the mass flow rate must increase in order to provide the same amount of thermal power to the users.
- The impact of partial load on the COP of chillers is taken into account in the case of individual chillers, but it is neglected in the case of centralized chillers. Indeed, district cooling systems have always multiple chillers being operational at anytime, thus avoiding shifting too far from design conditions.
- At most one storage technology can be installed in each plant.
- Sensible thermal energy storage is charged using chilled water at the network supply temperature, while ice and PCM thermal storages require cooling power at −5 °C and 3 °C, respectively.
- The model is based on a typical day and the operation costs are evaluated by multiplying the daily costs with the total number of utilization days, equal to 365 as the system is located in a tropical region where cooling is required all the year. In addition, an actualization coefficient is applied in order take into account the discount rate and the lifetime of the system, assumed equal to 30 years.

2.2. Master problem

2.2.1. Variables

The master problem is characterized by three different types of decision variables. The first group is formed by the integer variables x_u, which indicate by which plant the demand of the building u is satisfied. These can range from zero to the number of possible plant positions. The values assumed by these variables are therefore indices pointing to specific plant sites. If the variable x_u is equal to zero, instead it means that the building u is not connected to the network and that an individual cooling system is installed. The second group includes continuous variables named $vmax_m$, which indicate the velocity limit for every commercial diameter. These are used therefore to select the pipe diameters, after the evaluation of the mass flow rates. Finally, the last group is characterized by only one continuous variable, $\theta_{ch,s}$, which indicates the supply temperature of the network. Its upper bound depends on the supply temperature of the secondary loop, as it is assumed that the temperature difference at the pinch-point must be greater than 2 °C for technical reasons.

2.2.2. Cost function

The objective is to minimize the sum of capital and operation expenditures, characterized by the following terms.

- Investment and space occupancy cost of centralized and individual chillers
- Operating costs of centralized and individual chillers
- Investment and space occupancy costs of thermal storages
- Piping costs and energy transfer stations
- Pumping costs

Individual chillers are the ones installed in buildings not connected to the network, while centralized chillers are the ones installed in the plants of the district cooling network. The investment and operation costs of individual chillers can be directly computed, once the master problem variables are set. The capital and space occupancy costs of individual chillers installed in the buildings not connected to the district cooling network are computed as defined in Eqs. (1) and (2):

$$cost^{cap}_{ch,ind} = \sum_{u|x_u=0} c^u_{chill,ind} \tag{1}$$

$$cost^{occ}_{ch,ind} = \sum_{u|x_u=0} s^u_{ch,ind} * c_{occ} * \sum_{n=1}^{N_y} \frac{1}{(1+r)^n} \tag{2}$$

where $c^u_{chill,ind}$ is the capital cost of the chillers to be installed in building u, $s^u_{ch,ind}$ is the space occupied by the chiller and c_{occ} is the yearly cost of space occupancy per unit of surface, while the terms needed to compute the actualization factor, r and N_y, are the interest rate and the lifetime of the investment, respectively. The sizes of the individual chillers that would be installed in buildings not connected to the network are considered as a parameter as they are known a priori, since they depend only on the peak demand of these buildings. What is unknown is whether these chillers are installed or not, which depends on the values of the variables x_u, as they are installed only in buildings not connected to the network. As a consequence, the condition $x_u = 0$ is used to include in the summation only the buildings not connected to the district cooling network. The operating costs of individual chillers depend on the cooling energy produced in every time interval, the COP, the cost of electricity, the number of days the system is operative, the discount rate and the system lifetime. They are evaluated as defined in Eq. (3):

$$cost^{op}_{ch,ind} = \sum_{u|x_u=0} \sum_{t}^{T} Q^t_u / COP^t_u * c^t_{el} * \Delta t * n_d * \sum_{n=1}^{N_y} \frac{1}{(1+r)^n} \tag{3}$$

where Δt is the length of the time-step expressed in hours, Q^t_u is the cooling demand of building u at time t, while COP^t_u and c^t_{el} are the coefficient of performance of the chiller and the cost of electricity at time t, respectively. The COP indeed depends on the chiller load and on the outdoor temperature, which differs between day and night. The cost of electricity is also function of time, since the tariff is different during peak and off-peak hours.

The other cost terms can instead be evaluated only after having solved the subproblems. The solutions of the capacity and operation optimization subproblems (Section 2.3) provide the operating and the investment costs of centralized chillers and thermal storages installed in each plant site. Piping and pumping costs are computed once the topology is optimized (Section 2.4). Indeed, being the resulting network tree-shaped, the mass flow rates flowing in each branch can be evaluated by solving the linear system of mass balance equations defined in Eq. (4):

$$A * G^t = -G^t_{ext} \qquad \forall t \in T \tag{4}$$

where A is the incidence matrix of the tree network, G^t is a vector of mass flow rates flowing in each branch at time t and G^t_{ext} is the vector of mass flow rates entering into or exiting from the network. After the mass flow rates are computed, for each branch it is selected the smallest feasible commercial diameter for which the flow velocity is lower than the specified limit $vmax_m$, which is defined when setting the master problem variables. This is equivalent to solving the constrained optimization problem defined in Eq. (5):

$$\min \sum_{m}^{M} z^m_{ij} * D^m \qquad s.t.: \qquad \frac{\max_t G^t_{ij} * 4}{\pi * D^2_m} * z^m_{ij} \le vmax_m \qquad \forall m \in M \tag{5}$$

where the variable z^m_{ij} is a binary variable that indicates if a pipe with diameter D^m is installed in the edge that connects the nodes i and j. Once the sizes of the diameters are determined, the costs for piping and energy transfer stations can be computed, as defined in Eq. (6):

$$cost_{piping} = \sum_{ij}^{E} \sum_{m}^{M} L_{ij} * z^m_{ij} * c^m_{pipe} + \sum_{u|x_u>0} c_{ETS,u} \tag{6}$$

where L_{ij} is the length of the generic branch (i, j) and c^m_{pipe} is the unitary cost of a pipe with commercial size m. $c_{ETS,u}$ represents the cost to install the energy transfer station in building u and depends on its peak demand. The condition $u|x_u > 0$ is used to include in the summation only the buildings which are connected to the network. The pressure drops are computed as defined in Eq. (7)

$$\Delta p^t_{ij} = f * \frac{{G^t_{ij}}^2}{L_{ij} \rho D^4_{ij} / 8 * \pi^2} \qquad \forall (i,j) \in E, t \in T \tag{7}$$

where f is the friction coefficient, Δp^t_{ij} is the pressure drop on the generic branch (i, j) at time instant t and D_{ij} is the diameter of the pipe installed in that branch. Once the pressure drops are computed, the pumping power required by the pumps can be evaluated multiplying the mass flow rates with the pressure increase required by each pump.

$$P^t_{pump,w} = \frac{G^t_{ext,w} * \Delta p^t_{pump,w}}{\rho} \qquad \forall w \in H, t \in T \tag{8}$$

where $\Delta p^t_{pump,w}$ is the pressure increase required by the pump located at node w, $G^t_{ext,w}$ is the mass flow rate entering into the network from the node w and H is the set of possible plant nodes. The pressure increase is equal to the sum of pressure drops on the pipes of the most critical path, which is the path with the highest total pressure loss. Once pumping power needed by each pump is known, the total pumping cost is computed (Eq. (9)) by multiplying the pumping energy needed in each time interval with the cost of electricity, the number of operation days and the actualization coefficient, which depends on the discount rate r and system lifetime N_y.

$$cost_{pumping} = \sum_{w}^{H} \sum_{t}^{T} P^t_{pump,w} * \Delta t * c^t_{el} * n_d * \sum_{n=1}^{N_y} \frac{1}{(1+r)^n} \tag{9}$$

Table 1
Thermal storage properties [41].

Type	Cost	Latent heat [kJ/kg]	Density [kg/m^3]	Charging temperature [°C]	Life cycle [y]
Ice	50 €/m^3	334	917	−5	30
Commercial PCM	10 €/kWh	180	800	3	10
STES	50 €/m^3	0	1000	4–9	30

Table 2
Variables of design and operation of plant sites optimization subproblem.

Variable	Description	Unit
$Q^t_{ch,w}$	Compression chiller cooling power	kW
$Q^t_{abs,w}$	Absorption chiller cooling power	kW
$Q^t_{PCM,w}$	Cooling power stored/released by PCM thermal storage at time t	kW
$Q^t_{STES,w}$	Cooling power stored/released by sensible thermal storage at time t	kW
$Q^t_{Ice,w}$	Cooling power stored/released by ice thermal storage at time t	kW
$x^t_{PCM,w}$	Binary variable that indicates if PCM is charged at time t	/
$x^t_{Ice,w}$	Binary variable that indicates if Ice thermal storage is charged at time t	/
$C^t_{STES,w}$	Residual capacity of sensible thermal energy storage at time t	kWh
$C^t_{PCM,w}$	Residual capacity of PCM thermal storage at time t	kWh
$C^t_{Ice,w}$	Residual capacity of ice thermal storage at time t	kWh
$S_{STES,w}$	Sensible thermal storage maximum capacity	kWh
$S_{PCM,w}$	PCM thermal storage maximum capacity	kWh
$S_{Ice,w}$	Ice thermal storage maximum capacity	kWh
$N_{abs,w}$	Number of installed absorption chillers	/
$N^k_{ch,w}$	Number of installed chillers of size k	/
$N^k_{ch,st,w}$	Number of chillers of size k usable to produce chilled water at lower temperatures	/
$Q^t_{ch0,w}$	Cooling power produced by chillers in the form chilled water at $\theta_{ch,s}$	kW
$Q^t_{ch,PCM,w}$	Cooling power produced by chillers at time t at the temperature level required to charge PCM thermal storage	kW
$Q^t_{ch,Ice,w}$	Cooling power produced by chillers at time t at the temperature level required to charge ice thermal storage	kW
$MaxQ_{ch,st,w}$	Maximum chiller power producible at lower temperature levels	kW
$y_{PCM,w}$	Binary variable that indicates if PCM thermal storage is installed	/
$y_{STES,w}$	Binary variable that indicates if sensible storage is installed	/
$y_{Ice,w}$	Binary variable that indicates if ice thermal storage is installed	/

2.3. Capacity and operation optimization of chillers and storages

One of the subproblems to be solved is the optimization of the capacity and operation of chillers and storages. The chiller positions and the cooling demand they supply are determined through the master problem variables, while the optimal size and operation of chillers and storages in each plant are found by solving an MILP subproblem. The MILP model selects the quantity of chillers to install choosing from different types that have different capacities. In addition, absorption chillers may also be installed, if waste heat is available in the plant site. The storage size and the technology type are also selected by the model, choosing between ice, a commercial PCM, and sensible thermal storage. Ice and PCM are characterized by higher volumetric capacity, thanks to the latent heat, but they require lower supply temperatures during the charging phase, lowering the overall performances of chillers. In addition, ice storage is cheaper and has a longer life-cycle than commercial PCMs, which instead are often subjected to hysteresis and degradation. On the other hand, an advantage of PCMs is that they are available for almost any desired temperature range [40]. The main properties of the three technologies considered in this study are all reported in Table 1.

2.3.1. Variables

The model variables are described in Table 2. The hourly cooling demand and the network supply temperature instead are input parameters, as they are set when assigning the values of the master problem variables.

2.3.2. Cost function

The objective of this optimization subproblem is to minimize the sum of capital and operation expenditures of chillers and storages in each plant site. These are characterized by the following costs:

- chillers capital cost
- chillers space occupancy cost
- storage capital cost
- storage space occupancy cost
- chillers operation cost

The capital cost of centralized chillers depends on the number of installed chillers and their capacity, as defined in (10). In this analysis, we considered four possible capacities for compression chillers and one capacity for absorption chillers. However, this can be changed depending on the case study requirements. The capital cost of chillers installed in the generic plant site w is defined in Eq. (10)

$$cost^{cap}_{ch,w} = \sum_{k}^{K} N^k_{ch,w} * c_k + N_{abs,w} * c^{cap}_{abs} \tag{10}$$

where c_k is the capital cost to install a compression chiller of size k, $N^k_{ch,w}$ is the integer variable referring to the number of chillers of size k to be installed in the plant w, while c^{cap}_{abs} is the capital cost to install an absorption chiller and $N_{abs,w}$ is the number of absorption chillers to be installed. The cost of space occupancy of these chillers is defined in Eq. (11) and depends on the surface occupied by all the installed chillers.

$$cost^{occ}_{ch,w} = (\sum_{k}^{K} N^k_{ch,w} * s_k * + N_{abs,w} * s_{abs}) * c_{occ} \sum_{n=1}^{N_y} \frac{1}{(1+r)^n} \tag{11}$$

where s_k and s_{abs} refer to the space occupied by compression chillers of size k and by absorption chillers. Similarly, the capital and space occupancy cost of thermal storages depend on the installed storage technologies and their capacities. They are evaluated as defined in Eqs. (12) and (13):

$$cost^{cap}_{st,w} = S_{PCM,w} * c_{PCM} + S_{Ice,w} * c_{Ice} + S_{STES,w} * c_{STES} \tag{12}$$

$$cost^{occ}_{st,w} = (S_{PCM,w} * s_{PCM} + S_{Ice,w} * s_{Ice} * + S_{STES,w} * s_{STES}) * c_{occ} * \sum_{n=1}^{N_y} 1/(1+r)^n \tag{13}$$

where $S_{PCM,w}$, $S_{ICE,w}$ and $S_{STES,w}$ refer to the installed capacity of PCM, ice and sensible thermal storage in plant w, while c_{PCM}, c_{ICE} and c_{STES} refer to the unitary capital cost of these storages. The terms s_{PCM}, s_{STES} and s_{Ice} refer to the specific space occupancy of thermal energy storages per unit of capacity, expressed in m^2/kWh.

The operation cost of the chillers depends on the amount of cooling energy produced at the different temperature levels in each time interval and is defined as:

$$cost^{op}_{ch,w} = (\sum_{t}^{T}(\frac{Q^t_{ch,0,w}}{COP^t_0} + \frac{Q^t_{ch,PCM,w}}{COP^t_{PCM}} + \frac{Q^t_{ch,Ice,w}}{COP^t_{Ice}}) * \Delta t * c^t_{el} + Q^t_{abs,w} * \Delta t * c^{OM}_{abs}) * n_d * \sum_{n=1}^{N_y} \frac{1}{(1+r)^n} \quad (14)$$

where COP^t_0, COP^t_{PCM}, COP^t_{Ice} refer to the COP of the chillers when producing chilled water at supply temperatures respectively of: network, PCM and ice thermal storage. The COP is also dependant on the time instance, since during the night, the cooling water temperature in the condenser can decrease thanks to lower outdoor temperatures. The terms $Q^t_{ch,0,w}$, $Q^t_{ch,PCM,w}$, $Q^t_{ch,Ice,w}$ refer to the cooling power produced by the chillers when they supply water at nominal temperature and when charging PCM or ice thermal storage. The cost of electricity is defined by c^t_{el} and varies with time, since there are different tariffs for off-peak and peak hours. $Q^t_{abs,w}$ refers to the cooling power produced by absorption chillers, while c^{OM}_{abs} is the cost for operation and maintenance of absorption chillers per unit of cooling energy produced.

2.3.3. Constraints

The model constraints are mainly energy balance equations or capacity constraints. Eq. (15) is an energy balance constraint needed to ensure that the sum of the cooling power produced by the chillers, absorbed/released by the storages is equal to the cooling power requested by the buildings.

$$Q^t_{ch,w} + Q^t_{abs,w} + Q^t_{PCM,w} + Q^t_{Ice,w} + Q^t_{STES,w} = Q^t_w \quad \forall t \in T \quad (15)$$

where $Q^t_{ch,w}$, $Q^t_{PCM,w}$, $Q^t_{Ice,w}$, $Q^t_{STES,w}$ refer to the cooling power produced by the chillers, absorbed or released by PCM, ice or sensible thermal storages, respectively. Q^t_w is the total cooling demand that the plant w must satisfy at time t. It is given by the sum of the cooling demands of all the buildings that are fed by the plant w, which depend on the values of the x_u variables (Eq. (16))

$$Q^t_w = \sum_{u|x_u=w}^{U} Q^t_u \quad \forall t \in T \quad (16)$$

Constraints (17)–(19) are energy conservation equations, indicating that the residual storage capacity at time t depends on the storage capacity at the previous time-step and on the cooling energy absorbed or released by storages in the time interval between the two time-steps.

$$C^t_{PCM,w} = C^{t-1}_{PCM,w} - Q^t_{PCM,w} * \Delta t \quad \forall t \in T \quad (17)$$

$$C^t_{Ice,w} = C^{t-1}_{Ice,w} - Q^t_{Ice,w} * \Delta t \quad \forall t \in T \quad (18)$$

$$C^t_{STES,w} = C^{t-1}_{STES,w} - Q^t_{STES,w} * \Delta t \quad \forall t \in T \quad (19)$$

where $C^t_{PCM,w}$, $C^t_{Ice,w}$ and $C^t_{STES,w}$ are the capacities at time t of PCM, ice or sensible thermal energy storages. Inequality constraints (20)–(22) indicate that the residual storage capacity must not exceed the installed storage capacity.

$$C^t_{PCM,w} \leq S_{PCM,w} \quad \forall t \in T \quad (20)$$

$$C^t_{Ice,w} \leq S_{Ice,w} \quad \forall t \in T \quad (21)$$

$$C^t_{STES,w} \leq S_{STES,w} \quad \forall t \in T \quad (22)$$

Constraint (23) indicates that cooling power produced by compression chillers must not exceed the total installed chiller capacity.

$$Q^t_{ch,w} \leq \sum_{k}^{k} N^k_{ch,w} * S^k_{ch,w} \quad \forall t \in T \quad (23)$$

Constraint (24) is a big-M constraint that ensures that the cooling power produced at the temperature level required by PCM(3 °C) is null, if the PCM thermal energy storage is not charged at time t.

$$Q^t_{ch,PCM,w} \leq F * x^t_{PCM,w} \quad \forall t \in T \quad (24)$$

where F is a sufficiently large number at least equal to the upper bound of $Q^t_{ch,PCM,w}$, while $x^t_{PCM,w}$ is a binary variable that indicates if the PCM thermal storage is charging. Similarly, constraint (25) ensures that the cooling power produced at −5 °C is equal to zero if ice thermal storage is not charging.

$$Q^t_{ch,Ice,w} \leq F * x^t_{Ice,w} \quad \forall t \in T \quad (25)$$

where $x^t_{Ice,w}$ is a binary variable that indicates if the ice thermal energy storage is charging at time t. Constraints (26) and (27) instead indicate that the amount of cooling energy stored by PCM or ice thermal storage must not exceed the cooling power produced by the chillers at the specific temperature levels required to charge these storages.

$$Q^t_{PCM,w} \leq Q^t_{ch,PCM,w} \quad \forall t \in T \quad (26)$$

$$Q^t_{Ice,w} \leq Q^t_{ch,Ice,w} \quad \forall t \in T \quad (27)$$

Constraint (28) ensures that the cooling power produced by the chillers to charge either PCM or ice thermal storages does not exceed the installed chiller capacity for this scope.

$$Q^t_{ch,PCM,w} + Q^t_{ch,Ice,w} \leq \sum_{k}^{K} N^k_{ch,st,w} * S^k_{ch,w} \quad \forall t \in T \quad (28)$$

where $N^k_{ch,st,w}$ is the number of chillers of size k installed to charge PCM or ice thermal energy storages. Constraint (29) indicates that the installed chillers used to charge PCM or ice thermal energy storages are a subset of the total installed chillers.

$$N^k_{ch,st,w} \leq N^k_{ch,w} \quad \forall k \in K \quad (29)$$

Constraint (30) indicates that the cooling power produced in the form of chilled water at the network supply temperature must be lower or equal to the available capacity at time t. When neither PCM nor ice thermal storage is being charged, this capacity corresponds to the total one, while if either PCM or ice thermal storage is being charged, it corresponds to the installed chiller capacity that is not used to charge storages.

$$Q^t_{ch,0,w} \leq \sum_{k}^{K} (N^k_{ch,w} - N^k_{ch,st,w} * (x^t_{PCM,w} + x^t_{Ice,w})) * S^k_{ch,w} \quad \forall t \in T \quad (30)$$

The constraint is non-linear, since it includes the products between $N^k_{ch,st,w}$ and the variables $x^t_{PCM,w}$ and $x^t_{Ice,w}$. However, these are products between integer and binary variables and can be easily linearized by including additional variables and constraints as done in [29].

Constraint (31) ensures that the cooling power produced by absorption chillers does not exceed the amount of cooling that can be produced by absorption chillers. This depends on the available waste heat and on the COP of the absorption chillers.

$$Q^t_{abs,w} \leq Q^t_{waste-heat,w} * COP^t_{abs} \quad \forall t \in T \quad (31)$$

where $Q^t_{waste-heat,w}$ is the waste heat and COP^t_{abs} is the COP of the absorption chiller.

Constraint (32) ensures that the cooling power produced by absorption chillers does not exceed the installed capacity.

$$Q^t_{abs,w} \leq N_{abs,w} * S_{abs,w} \quad \forall t \in T \quad (32)$$

Constraint (33) limits to one the number of storage technologies installed in each plant.

$$y_{PCM,w} + y_{STES,w} + y_{Ice,w} \leq 1 \quad (33)$$

Constraints (34)–(36) ensure that the capacity of a storage is equal to zero, if that technology is not installed.

$$S_{PCM,w} \leq F * y_{PCM,w} \tag{34}$$

$$S_{Ice,w} \leq F * y_{Ice,w} \tag{35}$$

$$S_{STES,w} \leq F * y_{STES,w} \tag{36}$$

Constraint (37) is an energy balance indicating that the cooling power produced by chillers is equal to the sum of the cooling power produced at all temperature levels.

$$Q^t_{ch,w} = Q^t_{ch,0,w} + Q^t_{ch,PCM,w} + Q^t_{ch,Ice,w} \qquad \forall t \in T \tag{37}$$

Lastly, constraints (38)–(40) force the energy storages to complete full charge/discharge cycles everyday.

$$\sum_t^T Q^t_{PCM,w} = 0 \tag{38}$$

$$\sum_t^T Q^t_{STES,w} = 0 \tag{39}$$

$$\sum_t^T Q^t_{Ice,w} = 0 \tag{40}$$

2.4. Topology optimization subproblem

The second subproblem to be solved, once the master problem variables are set, is the network topology optimization. The optimization subproblem to be solved is also called Steiner tree problem and consists in finding the tree network that connects the selected chillers and buildings, minimizing the total network length. This is a generalization of the minimum spanning tree, since in this case, Steiner nodes (internal nodes) can be either included or not in the final network. On the other hand, when solving minimum spanning tree problems the Steiner nodes are always included. As a consequence, this subproblem is able to find a better solution, since the search space is wider. The problem is modelled as an MILP, where the cost function is represented by the total length, while the constraints are mass balances that ensure flow conservation in the network.

2.4.1. Variables

The model is characterized by the following four types of variables.

- A group of binary variables z^+_{ij} that indicate if the branch that connects node i with node j is selected and if the flow is directed from node i to node j.
- A group of binary variables z^-_{ij} that indicate if the branch that connects node i with node j is selected and if the flow is directed from node j to node i.
- A group of continuous non-negative variables $Gmax^+_{ij}$ that indicate the mass flow rate flowing from node i to node j
- A group of continuous non-positive variables $Gmax^-_{ij}$ that indicate the mass flow rate flowing from node j to node i.

The mass flow rates are therefore split in two groups of variables based on their flow directions.

2.4.2. Cost function

The objective of this model is to find the set of edges that constitute the tree network with the minimum total length and which connects the selected plants and buildings. The objective function is therefore given by Eq. (41)

$$L_{tot} = \sum_{ij}^{E} (z^+_{ij} + z^-_{ij}) * L_{ij} \tag{41}$$

where L_{tot} is the total length of the network, L_{ij} is the length of the generic branch that connects nodes i and j, while z^+_{ij} and z^-_{ij} are binary variables that indicate if branch (i, j) is selected and which flow direction.

2.4.3. Constraints

The constraints defined for this model are flow balances that guarantee the mass flow conservation in the network. Constraint (42) indicates that only one flow direction can be selected for each branch.

$$z^+_{ij} + z^-_{ij} \leq 1 \qquad \forall (i,j) \in E \tag{42}$$

If z^+_{ij} is equal to one, it means that the mass flows from i to j, while if z^-_{ij} is equal to one, it flows in the opposite direction. Constraints (43)–(44) enforce a mass flow rate to zero, if its branch is not selected in the final layout.

$$Gmax^+_{ij} \leq F * z^+_{ij} \qquad \forall (i,j) \in E \tag{43}$$

$$-Gmax^-_{ij} \leq F * z^-_{ij} \qquad \forall (i,j) \in E \tag{44}$$

where F is a sufficiently large number.

Constraint (45) ensures the mass balance in each node.

$$\sum_i^{V_j} Gmax^+_{ij} + Gmax^-_{ij} = Gmax^j_{ext} \qquad \forall j \in V \tag{45}$$

where $Gmax^j_{ext}$ is the maximum mass flow rate that is inserted or extracted from the network through node j. In internal nodes, no mass flow rate is extracted or inserted, so this quantity is equal to zero. For building nodes, it depends on if they are connected or not to the network, hence on the value of the master problem variables x_u. If they are disconnected, no flow is extracted, while if they are connected, the maximum extracted mass flow rate depends on the demand peak. For plant nodes, it instead depends on the sum of the demand peaks that they have to satisfy. As a consequence, they also depend on the values of the x_u variables. Eqs. (46) and (47) define how the external mass flow rate is calculated for buildings and plant nodes, respectively.

$$Gmax^u_{ext} = \frac{\max_t Q^t_u}{c_p * \Delta T} \qquad \forall u \in U | x_u > 0 \tag{46}$$

$$Gmax^w_{ext} = -\sum_{u|x_u=w} \frac{\max_t Q^t_u}{c_p * \Delta T} \qquad \forall w \in H \tag{47}$$

where ΔT is the temperature difference between supply and return and c_p is the specific heat.

3. Case study

The hierarchical framework described in the previous section has been applied to a Singaporean case study. The neighbourhood, object of the study, is a commercial district characterized by 18 buildings with a total cooling demand of 130 MW. Four possible plant positions have been considered, which are shown in Fig. 2 together with the neighbourhood topology and the position of the 18 buildings. The total demand curve of the neighbourhood is shown in Fig. 3. The demand reaches 40 MW during the night, since most buildings require cooling only during peak hours.

3.1. Scenarios

Eight different scenarios have been considered to study the feasibility of district cooling in a densely populated tropical area under different conditions. The scenarios differ from each others in terms of (i) indoor temperature set-point, (ii) availability of waste heat, (iii) COP of absorption chillers, (iv) electricity tariffs and (v) cost for space occupancy. The objective is therefore to determine how the optimal solution changes among the scenarios. Table 3 summarizes the different conditions that define the eight scenarios.

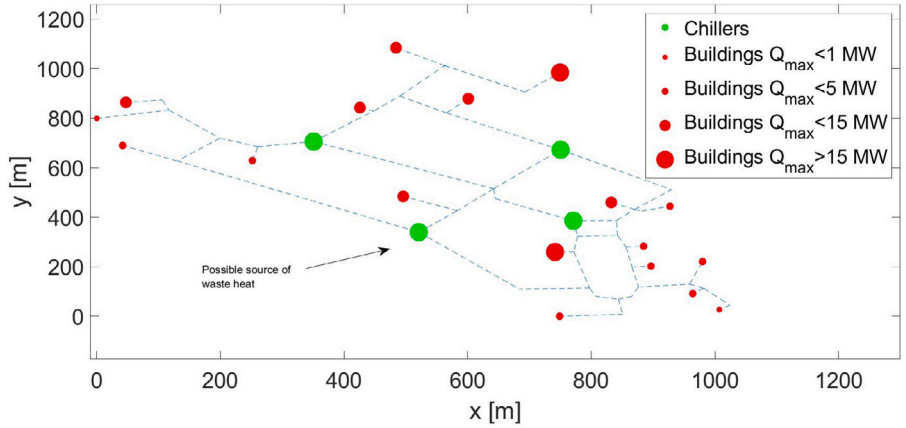

Fig. 2. Neighbourhood topology and possible chiller locations.

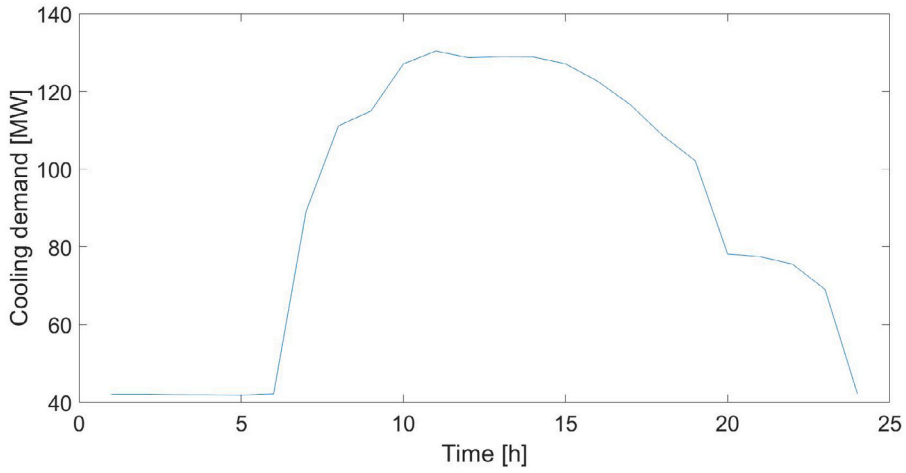

Fig. 3. Overall demand curve.

3.1.1. Scenario 1: Baseline

In the baseline scenario the indoor set-point temperature is assumed to be equal to 22.5 °C. The temperature difference between the indoor set-point and the entering airflow is assumed to be 11 °C, following ASHRAE standards [42]. As a consequence the air is cooled down to 11.5 °C. It is also assumed that 50% of indoor air is recirculated with outdoor air, in order to guarantee good air circulation. Outdoor air is assumed to have a temperature of 33 °C and relative humidity of 75%, as the design dry bulb temperature in Singapore is 33 °C [43], while relative humidity varies between 70% and 80%. The outdoor conditions are considered constant, although they vary throughout the day, as the objective is to determine the design conditions of the district cooling network. With these informations and assuming a logarithmic mean temperature difference of 5 °C between air and water in the air handling units, it is possible to fix the supply and return temperature of the chilled water in the secondary loops of the energy transfer stations. By varying the supply temperature of the district cooling network is therefore possible to compute the return temperature, fixing a logarithmic temperature difference of 3 °C between the primary and secondary loops. In this scenario no availability of waste heat is considered, while the electricity price is equal to 0.2 €/kWh in the peak hours and 0.12 €/kWh during off-peak hours [44]. Lastly, the space occupancy cost is considered equal to 70 €/(sqf*y) [34].

3.1.2. Scenario 2

In this scenario, it is assumed an indoor set point temperature of 25.5 °C, which is the upper limit according to Singaporean thermal comfort guidelines [45]. The motivation for the inclusion of this scenario is therefore to study the impact of a in increase of the indoor set-point temperature on the results. Thanks to the higher set-point temperature, the cooling demand decreases. A previous study found that for each Celsius degree increase in set-point temperature, the cooling demand decreases by 6% [46]. As a consequence, for this scenario it was considered a 18% lower cooling demand. In addition, the logarithmic temperature differences in the air handling units and in the substation heat exchanger are lowered by 18% as well, since the heat transfer areas are assumed to be equal to the baseline scenario. As a consequence, this leads to a higher upper bound of network supply temperature. Increasing the indoor set-point temperature therefore has a double positive impact, since cooling demand decreases and chillers can be operated at higher temperatures, with better performances.

3.1.3. Scenario 3,4,5,6

These scenarios are characterized by the availability of waste heat in one of the plant sites (Fig. 2). These scenarios have been therefore included with the goal of studying the benefits and the impact of waste heat utilization on the feasibility of district cooling networks. The scenarios differ from each other in terms of waste heat available and the COP of absorption chillers, which depends on the temperature of the waste heat source. In scenario 3 and 4 a waste heat of 10 MW is considered, while in scenario 5 and 6 the waste heat available is equal to 25 MW. Concerning the waste heat temperature, in scenarios 3 and 5, it is equal to 75 °C, while in scenarios 4 and 6 it is equal to 84 °C. In these scenarios, the indoor temperature set-point, the electricity tariff and the space occupancy cost are equal to the baseline scenario.

Table 3
Summary of scenarios conditions.

Scenario	Set point temperature [°C]	Cost of electricity [$/kWh]	Space occupancy cost	Waste heat
Baseline	22.5	Peaks: 0.2 €/kWh Off-peaks: 0.12 €/kWh	70 €/sqf	No
2	25.5	Peaks: 0.2 €/kWh Off-peaks: 0.12 €/kWh	70 €/sqf	No
3	22.5	Peaks: 0.2 €/kWh Off-peaks: 0.12 €/kWh	70 €/sqf	10 MW, T_{wh} = 75 °C
4	22.5	Peaks: 0.2 €/kWh Off-peaks: 0.12 €/kWh	70 €/sqf	10 MW, T_{wh} = 84 °C
5	22.5	Peaks: 0.2 €/kWh Off-peaks: 0.12 €/kWh	70 €/sqf	25 MW, T_{wh} = 75 °C
6	22.5	Peaks: 0.2 €/kWh Off-peaks: 0.12 €/kWh	70 €/sqf	25 MW, T_{wh} = 84 °C
7	22.5	Peaks: 0.28 €/kWh Off-peaks: 0.12 €/kWh	70 €/sqf	No
8	22.5	Peaks: 0.2 €/kWh Off-peaks: 0.12 €/kWh	Increasing 5% every year	No

Table 4
Main chillers parameters.

Typology	Capacity [MW]	Space occupancy [m^2]	Cost [M€]
Compression	0.5	28.68	0.23 [35]
Compression	1	31.45	0.45 [35]
Compression	3	44.16	0.9 [35]
Compression	10	89.38	4.5 [35]
Absorption	5	17.2	3.3 [47]

3.1.4. Scenario 7

Scenario 7 differs from the baseline in terms of electricity cost. The off-peak price does not change, while the peak price is assumed to be equal to 0.28 €/kWh. This scenario is included in the analysis with the objective of studying how the storage strategy changes with larger difference between off-peak and peak electricity prices.

3.1.5. Scenario 8

In scenario 8 it is assumed that the cost of space occupancy increases every year by 5%, while all the other parameters are the same as in the baseline. This scenario was considered, since most likely space occupancy cost will continue to increase in the future. The main objective is therefore to determine if the optimal storage technology changes if the occupancy cost will increase in the future.

3.2. Chillers parameters

In the analysis four types of compression chillers and one type of absorption chiller are considered. The main properties are reported in Table 4. The performance curves of the chillers were obtained consulting the library of the software DesignBuilder. They are bicubic or quadratic functions that express the nonlinear relation between COP and the partial load or the supply chilled water and condensing water temperature. More details regarding these functions are reported in the Appendix. Fig. 4(a) shows the bicubic performance curve of compression chillers as a function of supply and condensing water temperatures. Fig. 4(b) shows the bicubic curves of the COP as a function of the chiller load for the different chillers, setting the supply chilled water and condensing water temperatures to the standard ones (6.7 °C and 35 °C, respectively). As previously mentioned, the load curves were used only for individual chillers, since centralized ones tend to work more homogeneously, thanks to the installation of multiple chillers, which allows to minimize the effect of partial load. Fig. 4(c) shows the performance curves of absorption chillers as a function of chilled water temperature with two temperature levels of waste heat.

4. Results

In this section the results obtained from the application of the model to the Singapore case study are reported. The section is structured in six subsections that show the results in the different scenarios in terms of optimal topology, operation, storage technology, supply temperature, district cooling potential compared to traditional cooling and net present value. The master problem was solved by means of the genetic algorithm function of Matlab, while the solver Gurobi [48] was used to solve the MILP subproblems. The Dell Precision 7820 Tower with 96 Gb of RAM and the CPU Intel(R) Xeon(R) Gold 6230R 2.10 GHz was used to run all the simulations. The computational time ranges between 36 min and 3 h, depending on the scenario with an average of 2 h. The details regarding the computational time of the single scenarios are reported in Table 5.

Table 5
Computational time of the hierarchical model for different scenarios.

Scenario	Baseline	2	3	4	5	6	7	8
Computational time [s]	4220	3569	7500	9883	8319	9413	11 272	2163

4.1. Optimal topology

Fig. 5 shows the optimal topology in the different scenarios.

It can be observed that the number of connected buildings increases if the potential of district cooling compared to individual cooling is higher. Indeed, in the baseline scenario 12 buildings out of 18 are connected, while when absorption chillers are installed the number of connected buildings rises up to 16.

In most of the scenarios only one plant is installed. It is therefore preferred having a single larger plant, rather than multiple smaller ones. In scenarios 1, 3 and 8, the optimal plant location is the node with coordinates (771,385), as it is closer to most of the buildings, while in scenarios 3 and 4 the plant is placed in the node corresponding to the waste heat source. In scenario 5 and 6, more waste heat is available, allowing to connect additional buildings. Since the total capacity is larger in these scenarios, a second plant is also installed in order to better distribute the flow rates and consequently reduce the pumping costs.

In scenario 7, the solution consists in connecting 15 buildings and installing two independent networks, each fed by a chiller plant. The reason for this design is due to the need to reduce pumping costs, as they have a major weight if electricity price increases. In addition, in this scenario more buildings are connected with respect to the baseline, thanks to the larger savings achievable by district cooling when electricity is more expensive. In particular, the presence of cold storage allows to operate the chillers mainly during the off-peak hours, when electricity is less expensive.

It can be also observed that the building in the node with coordinates (740, 260) is never connected to the network in any scenario. The reason is that this building is a data centre with a cooling demand of 30 MW, hence already very efficient chillers can be installed there and they would always work at constant load, with high performances, since the data centre cooling demand is constant.

The results of this analysis therefore suggest that the parameters that most affect the topology of a district cooling network are the availability of free sources and the electricity price. In addition, a reduction of district cooling costs allows to connect more buildings, as it can be observed by comparing the baseline scenario with scenarios 2–6, where lower costs are achieved by either reducing the indoor set-point temperature or by exploiting waste heat sources.

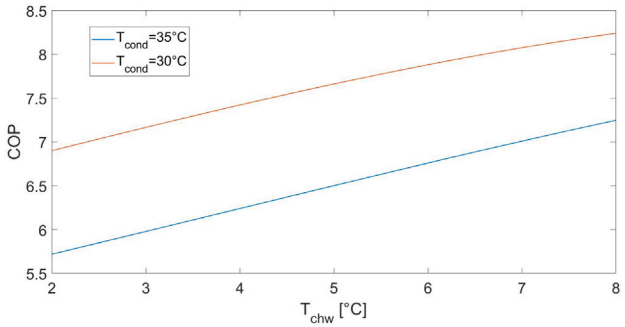

(a) Performance curve of compression chillers

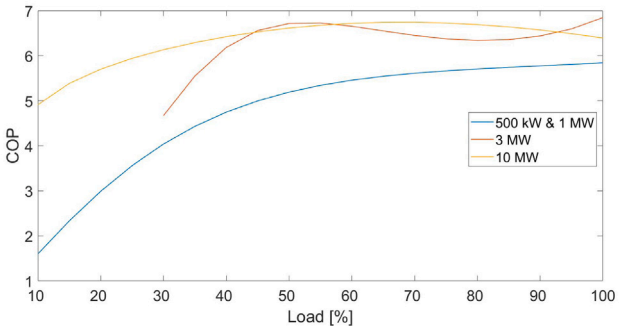

(b) COP in partial load conditions and T_{chw}=6.7°C and T_{cond}=35°C

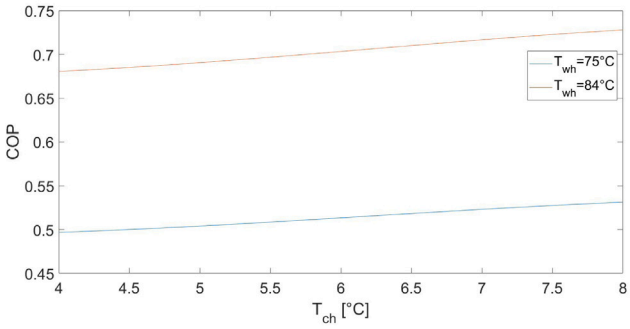

(c) Performance curves of absorption chillers

Fig. 4. Performance curves.

4.2. Comparison with individual cooling

Fig. 6 shows the cost comparison between the optimal solutions found by the model and two suboptimal solutions: one obtained connecting all buildings to the same chiller plant and the other refers to the case in which no district cooling is installed and all the buildings are cooled individually. In the baseline scenario, installing individual cooling systems in every building is 3.3% more expensive than the optimal solution. At the same time, connecting all the buildings to the network is 4.4% more expensive. The reason is that for some buildings it is more feasible installing individual cooling systems rather than being connected to a district cooling network. These differences between the three solutions change from one scenario to another, since the potential of district cooling depends the scenario conditions. When waste-heat is available (scenarios 3,4,5,6), the optimal solution is up to 16.5% less expensive than the one where all buildings are cooled individually. The electricity cost has also an impact on the potential of district cooling, as in scenario 7 the individual cooling solution is 7.6% more expensive than the optimal one.

These results hence highlight the importance of optimizing the buildings to connect, especially in the baseline scenario, where a non-optimized network would result more expensive than installing individual cooling systems in every building. In addition, the results underline the impact that electricity price and the availability of waste heat have on the feasibility of district cooling networks.

4.2.1. Levelized cost of individual cooling

The set of buildings to be connected to the district cooling network depends on the potential savings achievable compared to individual cooling. If the costs for individual cooling are already low, district cooling may not bring significant savings and may not be feasible. This is the case of some of the buildings of the case study, including the previously mentioned data centre. These buildings could be connected to the district cooling network if the selling price of cooling energy decreases, which is possible only if the district cooling costs are lowered(i.e. installing absorption chillers to exploit the available waste heat), or if individual cooling costs increase(i.e. increase of electricity cost). Fig. 7 shows the levelized cost of individual cooling for the 18 buildings in the baseline scenario. These are computed dividing the total individual cooling costs by the amount of cooling energy requested. The six points in red represent the buildings not connected to the network, which indeed are characterized by the lowest levelized costs and distances from the installed plant. The figure also suggests that the minimum selling price per unit of cooling energy should be greater than 0.039 €/kWh to make district cooling economically feasible. Lower selling prices would not cover the costs of this technology. The price could be decreased only by reducing district cooling costs(i.e. exploiting the waste heat through absorption chillers).

4.3. Optimal operation

Fig. 8 shows the optimal hourly operation in the different scenarios. In almost all scenarios, chillers are operated with almost constant load throughout the day, apart from the evening hours when they only produce the amount of cooling power demanded by the users. In the rest of the day, the cooling power produced is constant, while the storages are charged during the night, and discharged during the morning and afternoon hours. The lower cooling production during the evening hours is due to the fact that cooling demand is lower during these hours, but the electricity is more expensive, since the peak tariff is between 7 AM and 11 PM. Consequently it would not be convenient to operate the chillers with higher load to charge the storages. In scenario 7, the strategy is completely different, since the chillers are operated almost only during the night, due to the larger costs of electricity during peak hours, with respect to the baseline scenario; as a consequence, larger capacities of chillers and storages are installed. The operation strategy is therefore highly dependant on the difference between off-peak and peak electricity prices. In normal conditions, the following strategies can be adopted, based on the results:

- During peak hours, if the demand is lower than the average one, the chillers should provide only the cooling power requested by the storages.

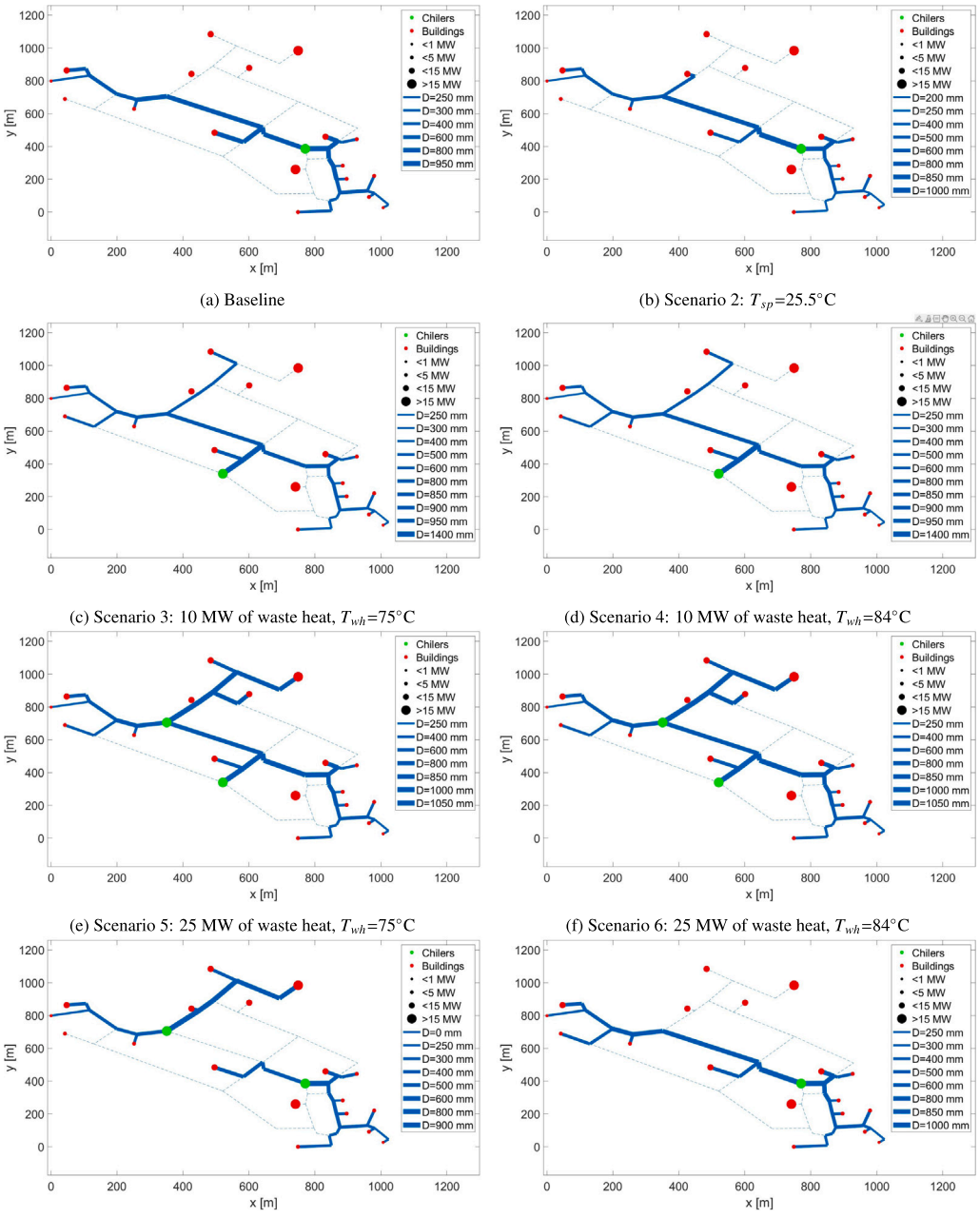

Fig. 5. Optimal topology in the different scenarios.

- In the rest of the day the chillers should be operated with a constant load and the storages shall be used for peak shaving and valley filling.

If there is a large difference between the tariffs, the strategy is instead to operate as much as possible the chillers during off-peak hours, in order to rely only on storages during peak hours.

4.4. Optimal storage technology

Fig. 9 shows the comparison between different storage solutions in each of the eight scenarios. The first three solutions *STES(heur.)*, *PCM (heur.)* and *ICE (heur.)* represent heuristic solutions obtained considering the installation of sensible, PCM or ice thermal storage, respectively. In addition, in these solutions the chillers are always operated with constant load, so the operation strategy is not optimized. It can be observed that the sensible thermal storage solution is the most expensive, due to the larger space occupation compared to PCM or ice thermal storage. The solutions *PCM(opt)* and *Ice(opt)* refer to solutions obtained considering PCM or ice thermal storage and no fixed operation strategy, contrarily to the previous three solutions. In these cases, the operation strategy and the design are combinedly optimized. Apart from scenarios 7 and 8, the differences between these solutions are around 1%, which means that in most cases PCM and ice thermal storages are almost equivalent in terms of overall costs. The reason is that the higher operation costs of chillers when producing ice are balanced by lower space occupation and longer life cycle. The results of these solutions are significantly different from the ones obtained with the heuristic assumption of constant chiller operation. Optimizing the size and operation of chillers and storage without this constraint allows to save from 4.2% to 27.5% in terms of total costs, depending on the scenario. The main reason is that if it is assumed an always

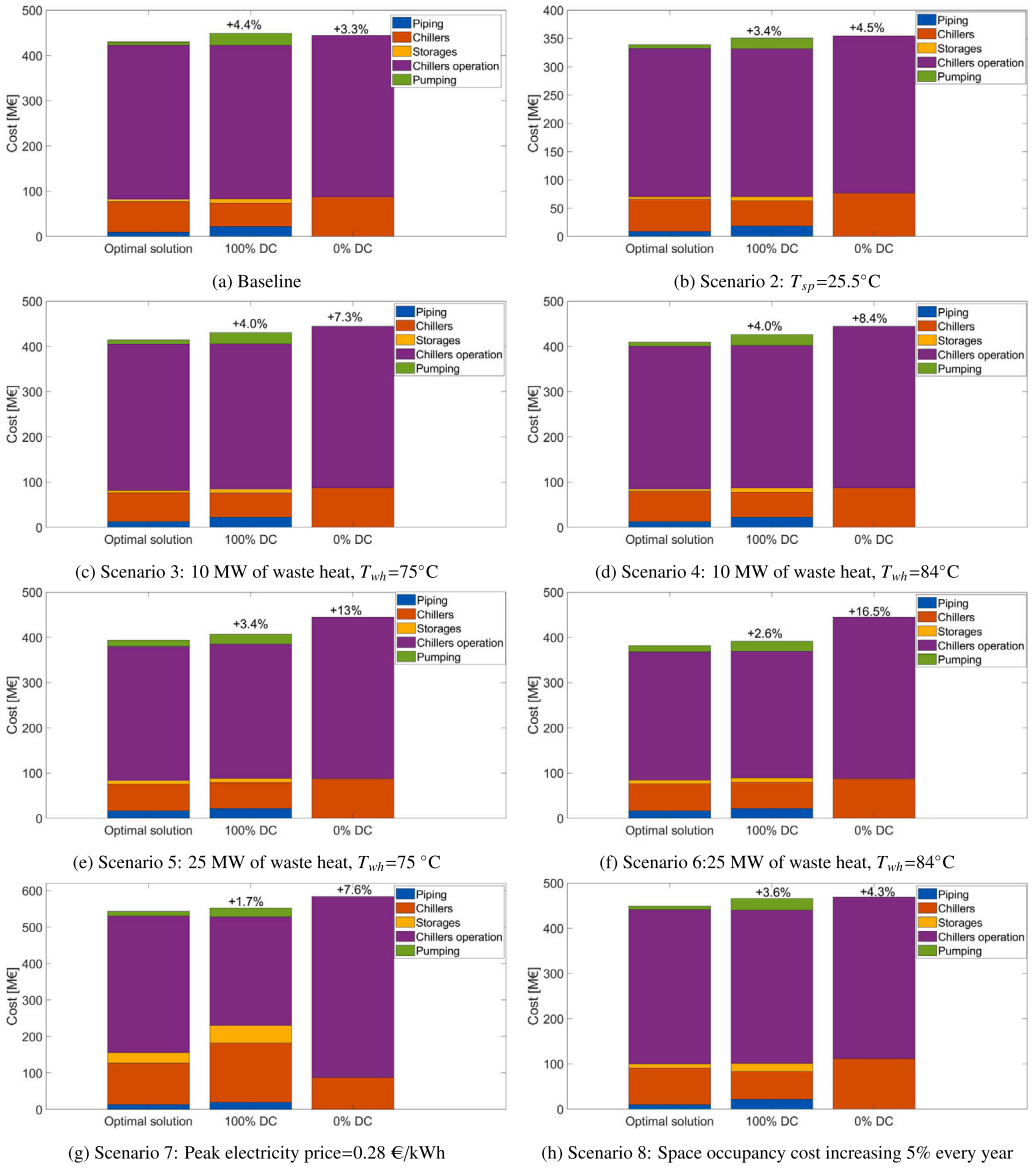

(a) Baseline

(b) Scenario 2: T_{sp}=25.5°C

(c) Scenario 3: 10 MW of waste heat, T_{wh}=75°C

(d) Scenario 4: 10 MW of waste heat, T_{wh}=84°C

(e) Scenario 5: 25 MW of waste heat, T_{wh}=75 °C

(f) Scenario 6:25 MW of waste heat, T_{wh}=84°C

(g) Scenario 7: Peak electricity price=0.28 €/kWh

(h) Scenario 8: Space occupancy cost increasing 5% every year

Fig. 6. Cost comparison with conventional cooling in the different scenarios.

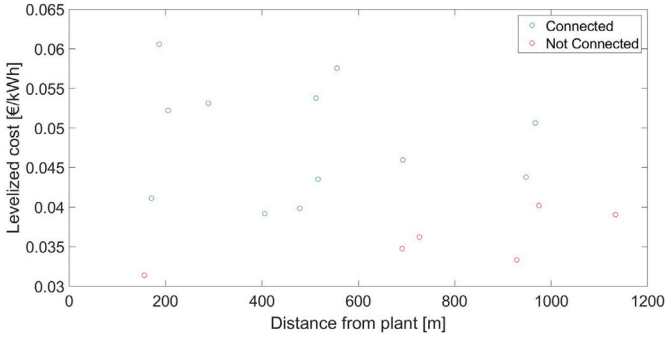

Fig. 7. Levelized cost of individual cooling for different buildings in the baseline scenario.

constant chiller operation, larger storages would be needed and they would be charged also when it is not convenient, such as during the evening hours(i.e. when the demand is lower than the average, but the electricity price is larger). In scenario 8, the difference between ice thermal storage and PCM optimal solutions is larger since the space occupancy cost increases by 5% every year. As a consequence, ice thermal storage results 3.6% cheaper since it is characterized by higher volumetric capacity. In scenario 7, the difference between ice thermal storage and PCM optimal solutions is also larger, since greater capacities are installed, due to the major price difference between peak and off-peak electricity prices. The figure shows also the benefits of thermal storage comparing the optimal solutions with ones lacking storage. In the baseline scenario, a district cooling network without a storage would be 9.1% more expensive in terms of total costs, since the chillers would be operated with higher loads during peak hours. This difference reaches 20.8% in scenario 7, where the electricity cost in peak hours is larger.

4.5. Optimal supply temperature

Fig. 10 shows the optimal supply temperature in the different scenarios. Apart from scenario 2 and 7, the optimal supply temperature is always around 5 °C. The optimal temperature is between the lower and

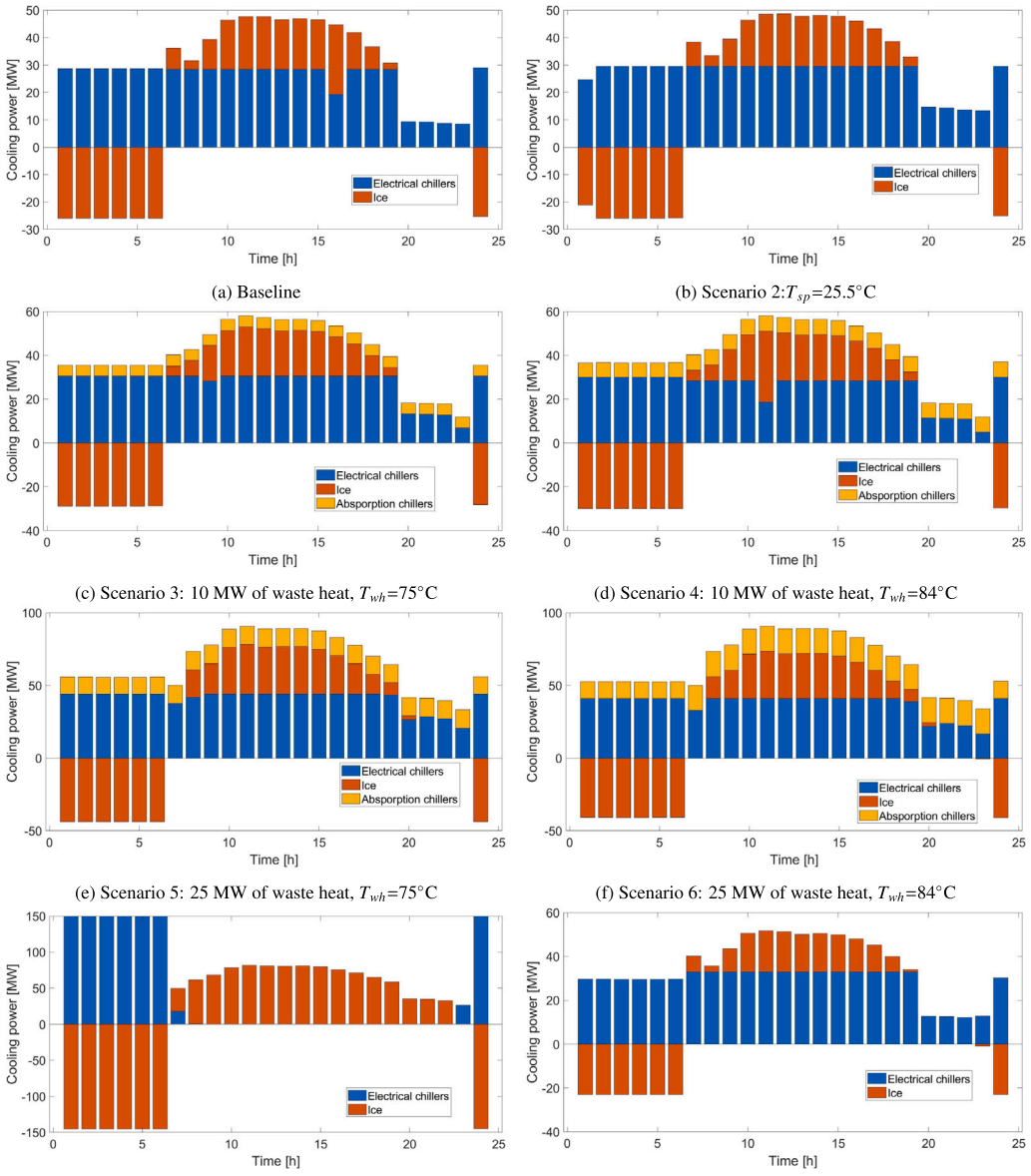

(a) Baseline

(b) Scenario 2:T_{sp}=25.5°C

(c) Scenario 3: 10 MW of waste heat, T_{wh}=75°C

(d) Scenario 4: 10 MW of waste heat, T_{wh}=84°C

(e) Scenario 5: 25 MW of waste heat, T_{wh}=75°C

(f) Scenario 6: 25 MW of waste heat, T_{wh}=84°C

(g) Scenario 7: $c_{el,peak}$=0.28 €/kWh

(h) Scenario 8: Space occupancy cost increasing 5% every year

Fig. 8. Optimal hourly operation in the different scenarios.

upper bounds, as it corresponds to the trade-off between pumping and chiller operation costs. Indeed, with a lower temperature, the chiller would operate at lower efficiency, but the temperature difference between supply and return would be higher, requiring lower mass flow rates and therefore lower pumping power. It can also be observed that when absorption chillers are used, the cost difference between the optimal supply temperature and the upper bound increases. The main reason is that the COP varies differently in compression and absorption chillers, due to different performance curves. In Scenario 7 the optimal supply temperature corresponds to the lower bound of 4 °C, since chillers are always operated to charge ice thermal storage at −5 °C. As a consequence, the chiller efficiency is already affected by that and supplying the network at a higher temperature has a minor impact on the coefficient of performance. The network is therefore operated at a temperature of 4 °C in order to minimize the pumping costs. Lastly, in scenario 2 the optimal supply temperature is higher, thanks to the higher indoor set-point temperature that enables the increase of the network supply and return temperatures.

4.6. Net present value analysis

In this subsection a Net Present Value analysis is presented, with the goal of determining:

- the economic benefits of increasing the indoor set-point temperature;
- the impact that waste heat has on the profitability and on the payback time of district cooling networks.

Fig. 11 shows the impact of increasing the indoor temperature set-point on the net present value and payback-time, by comparing scenario 2 with the baseline. In the analysis, the price of chilled water set by the utility represents the levelized cost for individual cooling, since that represents the threshold for the economical feasibility of district cooling. The results of the analysis show that by increasing by 3 °C the indoor temperature set-point, the payback time decreases from 14 to 11 years. In addition, with the increase of set point temperature, 43% higher NPV would be achieved at the end of lifetime. Increasing the indoor set-point temperature therefore leads to a higher profitability of district cooling. The result is not obvious, as the increase of

(a) Baseline

(b) Scenario 2: T_{sp}=25.5°C

(c) Scenario 3: 10 MW of waste heat, T_{wh}=75°C

(d) Scenario 4 10 MW of waste heat, T_{wh}=84°C

(e) Scenario 5: 25 MW of waste heat, T_{wh}=75°C

(f) Scenario 6: 25 MW of waste heat, T_{wh}=84°C

(g) Scenario 7: $c_{el,peak}$=0.28 €/kWh

(h) Scenario 8: Space occupancy cost increasing 5% every year

Fig. 9. Optimal storage technology in the different scenarios.

indoor set-point temperature causes a reduction of the cooling demand. On the other hand, the costs are reduced thanks to the lower supply temperature that allow to operate the chillers more efficiently. This results in higher revenues, which allow to reduce the payback time and increase the final NPV.

Fig. 12 compares the cashflow in baseline and in the scenarios where waste heat is available and exploited. It can be observed that if the waste heat available and the COP of the absorption chillers increase, the final net present value can increase by up to 3.5 times with respect to the baseline scenario thanks to the lower operating costs and larger number of users connected. Although the initial investments are higher, due to the larger installed capacity, in the scenarios where waste heat is exploited, the payback time is lower compared to the baseline. In particular, in scenario 6, the one characterized by the highest values of waste heat and source temperature, the paybacktime is 5 years lower than in the baseline. This result represents an additional proof to the potential impact that waste heat has on the feasibility of district cooling networks.

5. Discussion

The developed hierarchical method proved to effectively optimize different aspects regarding the design and operation of district cooling systems. The results obtained by applying the model to a Singapore neighbourhood case study not only highlighted the benefits of optimizing these parameters, but also showed how the optimal strategies could change in different scenarios and how further savings can be achieved with little changes in the everyday operation. In particular, it was shown that sensible thermal storage is not feasible in Singapore due to the extremely large cost of space occupancy. PCMs or ice thermal storages should instead be selected for their larger volumetric capacity, although they require lower temperatures to be charged. Moreover, if occupancy cost increases every year, ice thermal storage results being up to 3.6% more cost-effective than commercial PCM with operating temperatures. In addition, the operation strategy shall be properly optimized with the design, since it allows to sensibly reduce chiller operation and capital costs, compared to heuristic assumptions which

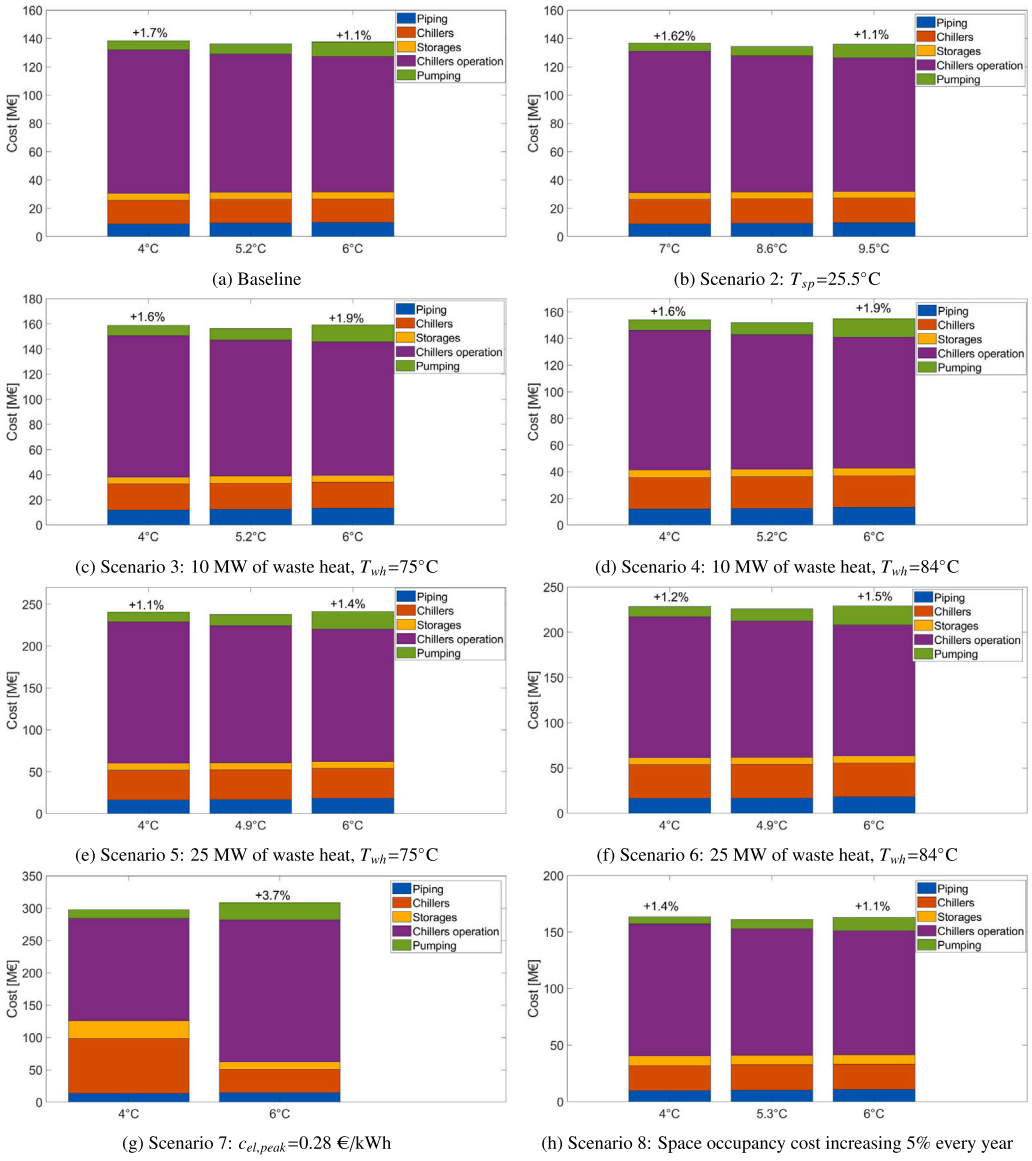

(a) Baseline

(b) Scenario 2: T_{sp}=25.5°C

(c) Scenario 3: 10 MW of waste heat, T_{wh}=75°C

(d) Scenario 4: 10 MW of waste heat, T_{wh}=84°C

(e) Scenario 5: 25 MW of waste heat, T_{wh}=75°C

(f) Scenario 6: 25 MW of waste heat, T_{wh}=84°C

(g) Scenario 7: $c_{el,peak}$=0.28 €/kWh

(h) Scenario 8: Space occupancy cost increasing 5% every year

Fig. 10. Optimal supply temperature in different scenarios.

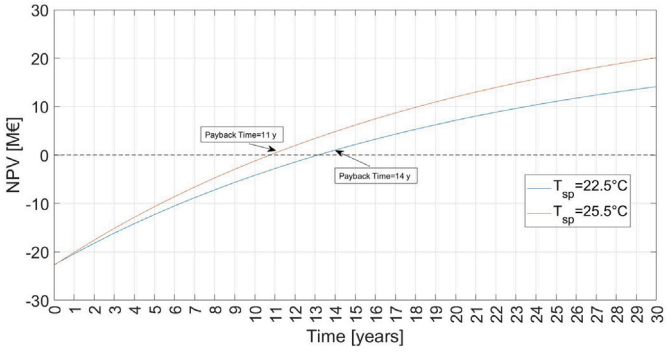

Fig. 11. Impact of indoor temperature set-point on the net present value and payback time.

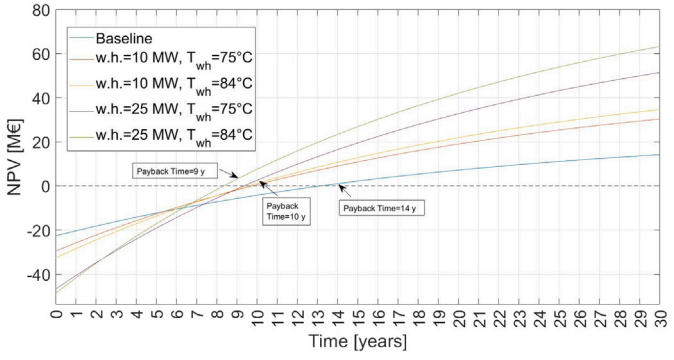

Fig. 12. NPV analysis in baseline scenario and with different quantities of available waste heat at different temperatures.

use fixed strategies. It was also showed that, in case the difference between off-peak and peak electricity price increases, the storage strategy would change drastically, as it would be more convenient to install larger chillers and storages in order to produce most of the daily cooling demand in the off-peak hours. In addition, it was shown that higher electricity costs tend to influence also the topology of the network, in order to minimize pumping costs. Secondly, it was shown that optimizing the network supply temperature allows to further reduce the

total costs, since there is a trade-off between pumping costs and chiller operation costs. The results indeed show that by increasing the network supply temperature, the chiller efficiency increases, but also the pumping costs, due to a lower temperature difference between supply and return line. The results also highlighted how the availability of waste-heat can significantly increase the potential of district cooling within a certain area, reducing the total costs, and lowering the payback time compared to the baseline scenario. Moreover, the use of waste heat would allow the further reduction of district cooling costs, making it a feasible option also for the buildings with low individual cooling costs.

5.1. Limitations and future studies

The main limitations of the proposed method depend on the assumptions under which it is based. In particular, it is assumed that each user's demand is consistently met by a single plant. While this assumption simplifies the problem, allowing to optimize separately each plant, it also reduces the exploration of the entire search space, thereby precluding the reaching of the global optimum. To address this limitation, future works should focus on the development of novel approaches capable of optimizing the cooling power dispatch from multiple plants and the flow distribution, with reasonable computational costs. In addition, considering the results obtained regarding the optimization of supply temperature, future research studies should also further explore this area. In particular, they should take into account the possible variation of supply temperature with time and outdoor conditions that differ from the design ones.

6. Conclusion

In this paper a novel hierarchical framework has been proposed for the design and operation optimization of district cooling networks. The hierarchical structure of the model allows to combinedly optimize a wide number of variables, including (i) the network topology, (ii) the position of plants, (iii) the capacity and hourly operation of chillers and storages, (iv) the storage technology to be installed, (v) the buildings to be connected to the network and (vi) the network supply temperature. The framework has been applied to a Singapore case study under eight different scenarios, each reflecting unique conditions such as indoor set-point temperature, waste heat availability, electricity cost during peak hours and space occupancy cost. The context of Singapore is indeed particularly interesting, since there is a large cooling demand all year round from both residential and commercial or office buildings. In addition, Singapore has a large population density and land scarcity. This makes district cooling attractive, but rises also the question regarding which is the most suitable storage technology. Several outcomes were obtained from the analysis:

- Increasing the set-point temperature by 3 °C can significantly increase the district cooling potential while reducing payback time of three year and increasing final NPV by 43%. This is achieved by lowering the users cooling demand and allowing the network to operate at a higher supply temperature, resulting in improved chiller performance.
- By exploiting waste heat through absorption chillers, district cooling potential can be significantly enhanced, with potential cost savings of up to 16.5% compared to conventional cooling systems. In the best-case scenarios, characterized by highest COP and available waste heat, NPV can increase by more than 350% and the payback time can be reduced from 14 to 9 years.
- Sensible thermal storage is not economically feasible, due to the extreme cost of space occupancy in Singapore. Instead, either ice or PCM thermal storage shall be adopted, with ice thermal storage proven to be the most cost effective option, especially in the context of rising space occupancy costs.
- The electricity tariffs significantly influence the optimal sizing and operation of chillers and storages within district cooling networks. The baseline scenario showed the importance of peak load reduction through homogeneous chiller operation, night-time storage charging, and daytime discharging. However, as the disparity between off-peak and peak electricity prices increases, it becomes more convenient to operate chillers exclusively at night and rely solely on storages during peak hours.
- The optimal network topology is highly influenced by electricity prices, due to the need to lower pumping costs, which have a higher impact. In particular, it could be convenient to install two independent district cooling networks to minimize pumping cost.

This hierarchical framework proposed represents a powerful tool for decision-makers involved in the task of designing and optimizing district cooling networks. Furthermore, by offering multiple outcomes and a fully optimized design and operation with minimal input parameters, this tool may both inspire future research studies or be used for planning future systems and clarify the DC potentials.

CRediT authorship contribution statement

Manfredi Neri: Writing – review & editing, Writing – original draft, Software, Methodology, Investigation, Formal analysis, Conceptualization. **Elisa Guelpa:** Writing – review & editing, Supervision, Resources, Methodology, Conceptualization. **Jun Onn Khor:** Writing – review & editing, Supervision, Resources, Methodology, Data curation, Conceptualization. **Alessandro Romagnoli:** Supervision, Resources, Methodology, Conceptualization. **Vittorio Verda:** Supervision, Resources, Methodology, Conceptualization.

Declaration of competing interest

The authors declare that they have no known competing financial interests or personal relationships that could have appeared to influence the work reported in this paper.

Data availability

The data that has been used is confidential.

Appendix. Chiller performance curves

In this appendix the mathematical formulation used to evaluate how the chiller performances change under different operating conditions is presented. The electrical power required by a chiller is evaluated as the power in design conditions multiplied by two correction factors f_{PLR} and f_T, which define how chillers performances change with partload, supply and condensation temperature.

$$P_{chiller} = P_{ref} * f_{PLR} * f_T \tag{A.1}$$

The partial load ratio PLR, defined in Eq. (A.2), represents the ratio between the cooling power produced by a chiller and the its available capacity.

$$PLR = Q_{chiller}/C_{chiller} \tag{A.2}$$

The coefficient of performance COP is the ratio between the cooling power produced by the chiller and electrical power required by it, so it is defined as:

$$COP = Q_{chiller}/P_{chiller} \tag{A.3}$$

which can also be written as (A.4), thanks to Eqs. (A.2) and (A.1).

$$COP = C_{chiller} * PLR/P_{ref} * \frac{1}{f_{PLR} * f_T} \tag{A.4}$$

Since the COP at full load is also defined as the ratio between $C_{chiller}$ and P_{ref}, Eq. (A.4) can also be reformulated as:

$$COP = COP_{ref} * \frac{PLR}{f_{PLR} * f_T} \quad (A.5)$$

As a consequence the COP under different operating conditions depends on the COP in design conditions and on the two correction factors. The partload correction factor f_{PLR}, defined in Eq. (A.6), is a bicubic function of load and the chiller condensation temperature.

$$f_{PLR} = a + b * T_{cond} + c * T_{cond}^2 + d * PLR + e * PLR^2 + f * PLR * T_{cond} + g * PLR^3 \quad (A.6)$$

If PLR is equal to 1 and the condensation temperature is the same as in standard conditions, f_{PLR} is also equal to 1. In these cases, the performances of the chiller depend only on the second correction factor. The supply temperature correction factor f_T, defined in (A.7), is a biquadratic function of supply and condensation temperature.

$$f_T = a + b * T_{cond} + c * T_{ch,s}^2 + d * T_{ch,s} + e * T_{ch,s}^2 + f * T_{cond} * T_{ch,s} \quad (A.7)$$

where the coefficients a, b, c, d, e, f and g are not equal in the two functions. They can be either provided by the manufacturer or obtained experimentally.

References

[1] International Energy Agency. Cooling. 2021, URL https://www.iea.org/reports/cooling.

[2] International Energy Agency. The future of cooling. 2018, URL https://www.iea.org/reports/the-future-of-cooling.

[3] Chow TT, Chan AL, Song CL. Building-mix optimization in district cooling system implementation. Appl Energy 2004;77:1–13. http://dx.doi.org/10.1016/S0306-2619(03)00102-8.

[4] Chan AL, Chow TT, Fong SK, Lin JZ. Performance evaluation of district cooling plant with ice storage. Energy 2006;31:2750–62. http://dx.doi.org/10.1016/J.ENERGY.2005.11.022.

[5] Inayat A, Raza M. District cooling system via renewable energy sources: A review. Renew Sustain Energy Rev 2019;107. http://dx.doi.org/10.1016/j.rser.2019.03.023.

[6] Zhang W, Jin X, Hong W. The application and development of district cooling system in China: A review. J Build Eng 2022;50:104166. http://dx.doi.org/10.1016/J.JOBE.2022.104166.

[7] Soltani M, Kashkooli FM, Dehghani-Sanij AR, Kazemi AR, Bordbar N, Farshchi MJ, Elmi M, Gharali K, Dusseault MB. A comprehensive study of geothermal heating and cooling systems. Sustainable Cities Soc 2019;44:793–818. http://dx.doi.org/10.1016/J.SCS.2018.09.036.

[8] Zhang W, Jin X, Zhang L, Hong W. Performance of the variable-temperature multi-cold source district cooling system: A case study. Appl Therm Eng 2022;213. http://dx.doi.org/10.1016/J.APPLTHERMALENG.2022.118722.

[9] Vandermeulen A, van der Heijde B, Helsen L. Controlling district heating and cooling networks to unlock flexibility: A review. Energy 2018;151:103–15. http://dx.doi.org/10.1016/J.ENERGY.2018.03.034.

[10] American Society of Heating Refrigeration and Air-Conditioning Engineers. District cooling guide. 2nd ed.. Atlanta: ASHRAE; 2019.

[11] Jangsten M, Lindholm T, Dalenbäck JO. Analysis of operational data from a district cooling system and its connected buildings. Energy 2020;203:117844. http://dx.doi.org/10.1016/J.ENERGY.2020.117844.

[12] Egberts P, Tümer C, Loh K, Octaviano R. Challenges in heat network design optimization. Energy 2020;203:117688. http://dx.doi.org/10.1016/J.ENERGY.2020.117688.

[13] Sameti M, Haghighat F. Optimization approaches in district heating and cooling thermal network. Energy Build 2017;140. http://dx.doi.org/10.1016/j.enbuild.2017.01.062.

[14] Gang W, Wang S, Xiao F, Gao DC. District cooling systems: Technology integration, system optimization, challenges and opportunities for applications. Renew Sustain Energy Rev 2016;53:253–64. http://dx.doi.org/10.1016/J.RSER.2015.08.051.

[15] Chiam Z, Easwaran A, Mouquet D, Fazlollahi S, Millás JV. A hierarchical framework for holistic optimization of the operations of district cooling systems. Appl Energy 2019;239:23–40. http://dx.doi.org/10.1016/J.APENERGY.2019.01.134.

[16] Yan B, Chen G, Zhang H, Wong MC. Strategical district cooling system operation with accurate spatiotemporal consumption modeling. Energy Build 2021;247:111165. http://dx.doi.org/10.1016/J.ENBUILD.2021.111165.

[17] Tang H, Yu J, Geng Y, Liu X, Lin B. Optimization of operational strategy for ice thermal energy storage in a district cooling system based on model predictive control. J Energy Storage 2023;62. http://dx.doi.org/10.1016/j.est.2023.106872.

[18] Chen Q, Wei W, Li N. Techno-economic control strategy optimization for water-source heat pump coupled with ice storage district cooling system. Int J Refrig 2022;138:148–58. http://dx.doi.org/10.1016/j.ijrefrig.2022.03.010.

[19] Cox SJ, Kim D, Cho H, Mago P. Real time optimal control of district cooling system with thermal energy storage using neural networks. Appl Energy 2019;238:466–80. http://dx.doi.org/10.1016/J.APENERGY.2019.01.093.

[20] Čož TD, Kitanovski A, Poredoš A. Exergoeconomic optimization of a district cooling network. Energy 2017;135:342–51. http://dx.doi.org/10.1016/J.ENERGY.2017.06.126.

[21] Guelpa E, Bellando L, Giordano A, Verda V. Optimal configuration of power-to-cool technology in district cooling systems. Proc IEEE 2020;108:1612–22. http://dx.doi.org/10.1109/JPROC.2020.2987420.

[22] Khir R, Haouari M. Optimization models for a single-plant District Cooling System. European J Oper Res 2015;247:648–58. http://dx.doi.org/10.1016/j.ejor.2015.05.083.

[23] Al-Noaimi F, Khir R, Haouari M. Optimal design of a district cooling grid: structure, technology integration, and operation. Eng Optim 2019;51. http://dx.doi.org/10.1080/0305215X.2018.1446085.

[24] Dorfner J, Krystallas P, Durst M, Massier T. District cooling network optimization with redundancy constraints in Singapore. Future Cities Environ 2017;3:1. http://dx.doi.org/10.1186/s40984-016-0024-0.

[25] Lambert RS, Maier S, Polak JW, Shah N. Optimal phasing of district heating network investments using multi-stage stochastic programming. Int J Sustain Energy Plan Manag 2016;9:57–74. http://dx.doi.org/10.5278/IJSEPM.2016.9.5, URL https://journals.aau.dk/index.php/sepm/article/view/1288.

[26] Shi Z, Hsieh S, Fonseca JA, Schlueter A. Street grids for efficient district cooling systems in high-density cities. Sustainable Cities Soc 2020;60:102224. http://dx.doi.org/10.1016/J.SCS.2020.102224.

[27] Neri M, Guelpa E, Verda V. Trade-off between optimal design and operation in district cooling networks. Smart Energy 2024;13. http://dx.doi.org/10.1016/j.segy.2023.100127, URL http://creativecommons.org/licenses/by/4.0/.

[28] Bordin C, Gordini A, Vigo D. An optimization approach for district heating strategic network design. European J Oper Res 2016;252:296–307. http://dx.doi.org/10.1016/J.EJOR.2015.12.049.

[29] Neri M, Guelpa E, Verda V. Design and connection optimization of a district cooling network: Mixed integer programming and heuristic approach. Appl Energy 2022;306. http://dx.doi.org/10.1016/j.apenergy.2021.117994.

[30] Neri M, Guelpa E, Verda V. Two-stage stochastic programming for the design optimization of district cooling networks under demand and cost uncertainty. Appl Therm Eng 2024;236:121594. http://dx.doi.org/10.1016/J.APPLTHERMALENG.2023.121594.

[31] Alghool DM, Elmekkawy TY, Haouari M, Elomri A. Optimization of design and operation of solar assisted district cooling systems. 2020, http://dx.doi.org/10.1016/j.ecmx.2019.100028.

[32] Ismaen R, Mekkawy TYE, Pokharel S, Al-Salem M. System requirements and optimization of multi-chillers district cooling plants. Energy 2022;246. http://dx.doi.org/10.1016/j.energy.2022.123349.

[33] Hsu C-Y, Lin T-Y, Liang J-D, Lai C-H, Chen S-L. Optimization analysis of waste heat recovery district cooling system on a remote island: Case study Green Island. 2019, http://dx.doi.org/10.1016/j.enconman.2019.01.028.

[34] Mazzoni S, Nastasi B, Ooi S, Desideri U, Comodi G, Romagnoli A. The adoption of a planning tool software platform for optimized polygeneration design and operation – A district cooling application in South-East Asia. Appl Therm Eng 2021;199. http://dx.doi.org/10.1016/J.APPLTHERMALENG.2021.117532.

[35] Zaw K, Kwik ZZ, Chang WQ, Islam MR, Poh TK. A techno-commercial decision support framework for optimal district cooling system design in tropical regions. Appl Therm Eng 2023;220. http://dx.doi.org/10.1016/J.APPLTHERMALENG.2022.119668.

[36] Gang W, Wang S, Augenbroe G, Xiao F. Robust optimal design of district cooling systems and the impacts of uncertainty and reliability. Energy Build 2016;122:11–22. http://dx.doi.org/10.1016/j.enbuild.2016.04.012.

[37] Wirtz M, Heleno M, Romberg H, Schreiber T, Müller D. Multi-period design optimization for a 5th generation district heating and cooling network. Energy Build 2023;284:112858. http://dx.doi.org/10.1016/j.enbuild.2023.112858.

[38] Wirtz M. nPro: A web-based planning tool for designing district energy systems and thermal networks. Energy 2023;268:126575. http://dx.doi.org/10.1016/J.ENERGY.2022.126575.

[39] He J, Guo Z, Li Y. Multi-objective optimization of district cooling systems considering cooling load characteristics. Energy Convers Manage 2023;281. http://dx.doi.org/10.1016/j.enconman.2023.116823.

[40] Souayfane F, Fardoun F, Biwole PH. Phase change materials (PCM) for cooling applications in buildings: A review. Energy Build 2016;129:396–431. http://dx.doi.org/10.1016/J.ENBUILD.2016.04.006.

[41] Hauer A. Thermal energy storage. 2013, URL https://iea-etsap.org/E-TechDS/PDF/E17IR%20ThEnergy%20Stor_AH_Jan2013_final_GSOK.pdf.

[42] Goel S, Rosemberg M, Eley C. ANSI/ASHRAE/IES standard 90.1-2016 performance rating method reference manual. 2017.

[43] Saber EM, Iyengar R, Mast M, Meggers F, Tham KW, Leibundgut H. Thermal comfort and IAQ analysis of a decentralized DOAS system coupled with radiant cooling for the tropics. Build Environ 2014;82:361–70. http://dx.doi.org/10.1016/J.BUILDENV.2014.09.001.

[44] SP group. Electricity tariff revision for the period 1 april to 30 june 2022. 2023, URL https://www.spgroup.com.sg/dam/spgroup/wcm/connect/spgrp/b37ad027-acf7-4951-a6c4-8d1d7c06c7de/%5B20220331%5D+Media+Release+-+Electricity+tariff+revision+for+the+period+1+April+to+30+June+2022.pdf?MOD=AJPERES&CVID=.

[45] Singaporean Building and Construction Authority. Code on environmental sustainability measures for existing buildings. 2016.

[46] Yamtraipat N, Khedari J, Hirunlabh J, Kunchornrat J. Assessment of Thailand indoor set-point impact on energy consumption and environment. Energy Policy 2006;34:765–70. http://dx.doi.org/10.1016/J.ENPOL.2004.07.009.

[47] US Department of Energy. Absorption chillers for CHP systems. 2017.

[48] Gurobi Optimization. Gurobi reference manual. 2023, URL https://www.gurobi.com.